T.R.
GEBZE TECHNICAL UNIVERSITY
GRADUATE SCHOOL OF SCIENCES

TEM WAVE PROPAGATION IN COAXIAL WAVEGUIDES WITH STEP DISCONTINUITY

HÜSEYİN SİNAN AKŞİMŞEK
A THESIS SUBMITTED FOR THE DEGREE OF
DOCTOR OF PHILOSOPHY
DEPARTMENT OF ELECTRONICS ENGINEERING

GEBZE
2014

T.R.
GEBZE TECHNICAL UNIVERSITY
GRADUATE SCHOOL OF SCIENCES

TEM WAVE PROPAGATION IN COAXIAL WAVEGUIDES WITH STEP DISCONTINUITY

HÜSEYİN SİNAN AKŞİMŞEK
A THESIS SUBMITTED FOR THE DEGREE OF
DOCTOR OF PHILOSOPHY
DEPARTMENT OF ELECTRONICS ENGINEERING

THESIS SUPERVISOR
ASSOC. PROF. DR. GÖKHAN ÇINAR

GEBZE
2014

GEBZE YÜKSEK TEKNOLOJİ ENSTİTÜSÜ	DOKTORA JÜRİ ONAY FORMU

GYTE Mühendislik ve Fen Bilimleri Enstitüsü Yönetim Kurulu'nun .....28/11/2014..... tarih ve ..2014../..66..... sayılı kararıyla oluşturulan jüri tarafından 05/12/2014 tarihinde tez savunma sınavı yapılan Hüseyin Sinan Akşimşek'in tez çalışması Elektronik Mühendisliği Anabilim Dalında DOKTORA tezi olarak kabul edilmiştir.

JÜRİ

ÜYE
(TEZ DANIŞMANI) : Doç. Dr. Gökhan Çınar

ÜYE : Prof. Dr. Ali Alkumru

ÜYE : Prof. Dr. Gökhan Uzgören

ÜYE : Doç. Dr. İsmail Hakkı Tayyar

ÜYE : Doç. Dr. Ahmet Demir

ONAY

GYTE Mühendislik ve Fen Bilimleri Enstitüsü Yönetim Kurulu'nun ..... tarih ve ...../..... sayılı kararı.

İMZA/MÜHÜR

SUMMARY

In this thesis, the propagation of TEM waves along a coaxial waveguide involving single step discontinuity on the outer wall and the inner wall is investigated in order to understand the nature and the effect of the area expansion on the scattering phenomenon. These two problems are independently analyzed by applying Wiener-Hopf and Mode-Matching techniques, both of which are considered to be rigorous analyses. First, each problem is examined by Wiener-Hopf technique. By applying Fourier integral transformation to Helmholtz equation and then taking into account the boundary conditions and the continuity relations in related transform domain, a modified Wiener-Hopf equation of the second type is obtained for each problem. The solution of each Wiener-Hopf equation is determined in terms of an infinite number of unknown coefficients, which satisfy an infinite set of linear algebraic equations. These systems are solved numerically and the related explicit statements are derived. Then, the Mode-Matching technique is applied to the problems. This method gives two infinite sets of equations for each geometry, and this pair of equations is solved simultaneously. Later, by using the explicit statements for each geometry and each technique, a computer program is coded in MATLAB, and the computational results are presented graphically for the related problems. The graphs show the effect of area ratio on the scattering coefficients in the case of TEM mode. The computational results are also examined considering the rate of convergence. It is observed that the Wiener-Hopf technique provides a better convergence than the Mode-Matching technique. At the final chapter of the thesis, all numerical results are evaluated in terms of each problem, and the Wiener-Hopf and Mode-Matching techniques are compared in terms of accuracy, computation time, and applicability in more complex problems.

Key Words: Coaxial, Waveguides, Discontinuities, Electromagnetic Wave Propagation, Electromagnetic Wave Scattering, Mode-Matching Technique, Wiener-Hopf Technique.

ÖZET

Bu çalışmada, önce dış duvarında ve ardından da iç duvarında basamak süreksizliği bulunan bir koaksiyel dalga kılavuzunda TEM dalgaların yayılımı incelenmiştir. Bu iki probleme, kesin çözüm yöntemi oldukları kabul edilen Wiener-Hopf ve Mod-Uydurma teknikleri ayrı ayrı uygulanmıştır. Her bir problem, öncelikle, Wiener-Hopf tekniği ile analiz edilmiş, bu doğrultuda Helmholtz denklemine Fourier dönüşümü uygulanmış, ardından sınır ve süreklilik koşulları aynı tanım alanında işleme sokularak her problem için 2. türden birer Modifiye Wiener-Hopf denklemi elde edilmiştir. Bu denklemlerin çözümü, sonsuz sayıda lineer cebirsel denklem sistemini sağlayan, sonsuz sayıda bilinmeyen katsayılar sistemi cinsinden elde edilmiştir. Bu sistemler sayısal olarak çözülmüş ve her sisteme ilişkin açık ifadeler türetilmiştir. Ardından, ilişkin problemlere Mod-Uydurma tekniği uygulanmıştır. Tekniğe özgü formülasyonun ardından, her problem için bir çift sonsuz denklemler sistemi elde edilmiş ve bu denklem çiftleri eşzamanlı olarak çözülmüştür. Analitik çalışmanın ardından, uygulanan iki tekniğin sonucunda her problem için elde edilen ifadeler kullanılarak, MATLAB programlama dilinde programlar yazılmış, problemler nümerik olarak çözülmüş ve sonuçlar üretilen grafikler ile sunulmuştur. Bu grafiklerden kimileri duvarlar arasındaki alan genişlemesinin her iki yöntemle elde edilen saçılma katsayılarına olan etkilerini ortaya koyarken, kimileri de kullanılan yöntemlerin yakınsaklık davranışlarını betimlemektedir. Bu bakımdan Wiener-Hopf tekniğinin, Mod-Uydurma tekniğinden çok daha hızlı yakınsadığı gözlenmiştir. Son bölümde, hesaplamalı sonuçlar her bir problem açısından değerlendirilmiş ve Wiener-Hopf ve Mod-Uydurma teknikleri doğruluk, hesaplama üstünlüğü ve karmaşık problemlerde uygulanabilirlik açılarından karşılaştırılmıştır.

Anahtar Kelimeler: Koaksiyel, Dalga Kılavuzları, Süreksizlikler, Elektromanyetik Dalga Yayılımı, Elektromanyetik Dalga Saçınımı, Mod-Uydurma Tekniği, Wiener-Hopf Tekniği.

ACKNOWLEDGEMENTS

This PhD thesis is the result of a challenging journey, upon which many people contributed and given their support. First and foremost, I am deeply indebted to my advisor Assoc.Prof.Dr.Gökhan Çınar for his fundamental role in my doctoral work. I would like to thank him for his guidance, patience and faith in me during my research. I would particularly like to acknowledge Prof.Dr.Gökhan Uzgören for his support, suggestions and encouragement during all my studies. I am deeply thankful to Assoc.Prof.Dr. İsmail Hakkı Tayyar for his time and valuable contributions on this thesis. I also would like to thank Prof.Dr. Ali Alkumru for the substantial influence that his courses have had on my research. I am very thankful to the members of Department of Electronics Engineering at Gebze Technical University.

I am deeply thankful to my family for their love, support, and sacrifices. Without them, this thesis would have never been written.

TABLE of CONTENTS

LIST of ABBREVIATIONS and ACRONYMS

Abbreviations and Acronyms		**Explanations**
FDTD	:	Finite Difference Time Domain
MWHE	:	Modified Wiener Hopf Equation
TEM	:	Transverse Electromagnetic
TM	:	Transverse Magnetic

LIST of FIGURES

1. INTRODUCTION

Waveguides are composite structures containing not only uniform or nonuniform regions, but also discontinuity regions [1] and electromagnetic wave propagation in waveguides has been an interesting topic and subject to various engineering problems, such as microwave and transmission line measurement techniques, filters, connectors, and matching devices. A typical example is with the low-frequency electromagnetic modelling of a power cable measurement setup [2], where there are many scattering mechanisms, such as different inner and outer radii of two connected coaxial cables, different dielectric media, etc. Among these mechanisms, scattering by step discontinuities in coaxial waveguides has been drawing interest since many decades, and considering the literature, there can be several different types of discontinuities. For instance, single step in one conductor is one of the most common problem which is referred to the abrupt step on the inner or outer conductor wall of a coaxial waveguide. A double step in both conductor walls occurs frequently in engineering applications as well similar to the previous type, and it can be characterized by a junction region of two connected coaxial cables which have different inner and outer radii. On the other hand, a longitudinal discontinuity, i.e., a gap on the inner conductor wall of a coaxial cable is related to a finite gap problem.

Step type discontinuity in a coaxial cable was first studied by Whinnery et al. in 1944 where they obtained an equivalent circuit by placing an admittance at the plane of discontinuity in the case of TM waves [3]. In 1965, Green analyzed different configurations of step discontinuity in coaxial waveguides numerically by use of finite difference technique [4]. Here, Green studied the finite gap discontinuity on the inner conductor wall and obtained a π-type equivalent circuit in static case for the representation of the gap. In 1998, Eom et al. obtained analytical series solution for scattering on the problem of a coaxial line terminated by a gap using the Fourier transform and the Mode-Matching technique [5]. In the same year, Mongiardo et al. analyzed the step type problem with generalized network formulation by the use of Green's function [6]. Yu et al. applied a nonuniform Finite Difference Time Domain (NUFDTD) technique to study cascaded circularly symmetric discontinuities on waveguides in 2001 [7]. In 2004, Obrzut et al. analyzed a coaxial line terminated by a gap numerically by the use

of the commercial simulator HFSS [8]. Finally, in 2006, Fallahi and Rashed-Mohassel considered the dyadic Green's function approach using the principle of scattering superposition for the problem where there is a step discontinuity on the inner wall [9]. Waveguide discontinuities with axial symmetry were successfully studied in time domain methods as well as in [10]-[12].

This thesis investigates the TEM wave propagation along a coaxial waveguides involving single step discontinuity on the outer and inner wall. These two problems are separately analyzed by applying both Wiener-Hopf and Mode-Matching techniques in order to understand the nature and the effect of the area expansion on the scattering phenomenon.

In chapter 2, first, the Wiener-Hopf technique is applied to the problem of step discontinuity on the outer wall by considering direct Fourier transform of the Helmholtz equation, boundary conditions, and continuity relations, and then a unique type of Wiener-Hopf equation is determined following a similar procedure mentioned in [13]-[17]. This is a modified Wiener-Hopf equation (MWHE) of the second type and it involves a certain kernel function characterizing the nature of the step discontinuity on the outer wall. The modified Wiener-Hopf equation is solved in terms of an infinite number of unknown coefficients, which satisfy an infinite set of linear algebraic equations, and then the scattering coefficients are obtained at the end of the analysis. The solution of this Wiener-Hopf equation has an importance in some engineering applications such as microwave filters and power-line measurements mentioned in [2]. The same problem is then analyzed by applying the Mode-Matching technique, as described in [16]. Mode-Matching technique is a well-known method for formulating boundary-value problems in guided-wave theory and it has been widely used in previous studies involving step discontinuities at waveguides in general [17]-[19] and at coaxial waveguides when the discontinuities exist both on inner and outer walls [20]-[21]. Following a similar procedure as described in [21], the scattering coefficients are determined at the last part of this chapter.

In chapter 3, the problem of step discontinuity on the inner wall is analyzed by applying both Wiener-Hopf and Mode-Matching techniques, following the same procedure as discussed in the previous chapter.

After determining the analytical results, a computer code is developed in MAT-

LAB for each problem and each technique. Chapter 4 deals with the numerical results involving the scattering parameters in the case of TEM mode. This chapter also presents the comparison of the Wiener-Hopf and Mode-Matching techniques computationally as well in terms of the accuracy and the speed of convergence, which has not been done before in the literature to the best of the author's knowledge. The related graphs in this chapter show that the Wiener-Hopf technique has a faster convergence than the Mode-Matching technique. Contrary to the Wiener-Hopf technique, the Mode-Matching technique does not take into account the edge condition, this lack causes the Mode-Matching technique converge slow.

This study is strongly motivated by engineering applications, in particular, power-line measurements mentioned in [2], and in chapter 5, all numerical results are evaluated in terms of practical applications. The comparison of the Wiener-Hopf and the Mode-Matching techniques provides an understanding for future studies involving more complex geometries.

Time dependence $exp(-i\omega t)$, with ω being the angular frequency is assumed and suppressed throughout the analysis. Conductor walls in both problems are perfect electric conductor (PEC) and the geometries don't involve any physical discontinuities.

2. STEP DISCONTINUITY ON THE OUTER WALL

2.1. Wiener-Hopf Analysis

2.1.1. Formulation of the problem

Consider a semi-infinite coaxial cylindrical waveguide whose inner and outer cylindrical walls are located at $\rho = a$ for $z \in (-\infty, 0)$ and $\rho = b$ for $z \in (-\infty, 0)$ is connected to another semi-infinite coaxial cylindrical waveguide whose inner and outer cylindrical walls are located at $\rho = a$ for $z \in (-\infty, \infty)$ and $\rho = d$ for $z \in (0, \infty)$ as illustrated in Figure 2.1.

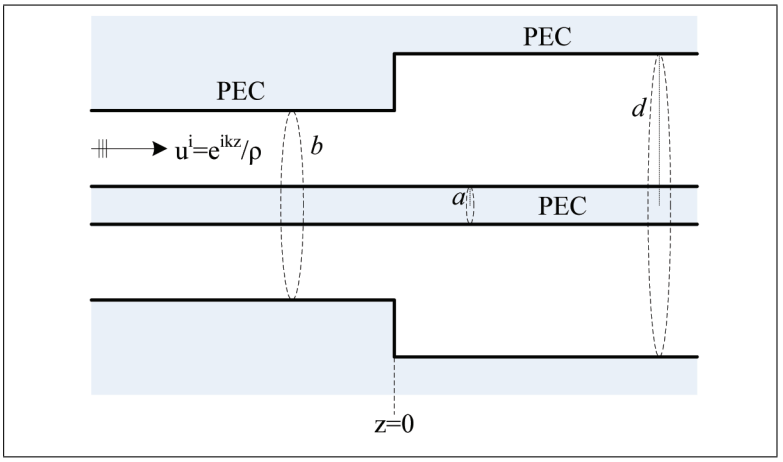

Figure 2.1: Geometry of the problem.

Let the incident TEM mode (with only a ϕ-component of the magnetic field and a ρ-component of the electric field being nonzero) propagating in the positive z direction be given by

$$H_\phi^i(\rho, z) = u_i(\rho, z) = \frac{e^{ikz}}{\rho} \tag{2.1}$$

where k is the propagation constant, which is assumed to have a small imaginary part corresponding to slightly lossy medium. The lossless case can then be obtained by letting $\mathrm{Im}(k) \to 0$ at the end of the analysis. In virtue of the axial symmetry of the

problem, all the field components may be expressed in terms of $H_\phi(\rho,z) = u(\rho,z)$ as follows:

$$E_\rho = \frac{1}{i\omega\epsilon}\frac{\partial}{\partial z}u(\rho,z) \quad \text{and} \quad E_z = -\frac{1}{i\omega\epsilon}\frac{1}{\rho}\frac{\partial}{\partial \rho}\left[\rho u(\rho,z)\right] \tag{2.2}$$

where the other components of the fields are zero. For the sake of analytical convenience, the total field $u_T(\rho,z)$ can be expressed as

$$u_T(\rho,z) = \begin{cases} u_i(\rho,z) + u_1(\rho,z) & , \quad a < \rho < b \\ u_2(\rho,z)\,H(z) & , \quad b < \rho < d \end{cases} \tag{2.3}$$

with $H(z)$ being the Heaviside step function and where $u_1(\rho,z)$ and $u_2(\rho,z)$ are the scattered fields which satisfy the Helmholtz equation

$$\left[\frac{\partial^2}{\partial\rho^2} + \frac{1}{\rho}\frac{\partial}{\partial\rho} + \frac{\partial^2}{\partial z^2} + \left(k^2 - \frac{1}{\rho^2}\right)\right] u_j(\rho,z) = 0 \quad , \quad j = 1,2 \tag{2.4}$$

for $j = 1,2$ in their domains of validity with the boundary conditions

$$u_1(a,z) + a\frac{\partial}{\partial\rho}u_1(a,z) = 0 \quad , \quad z \in (-\infty,\infty) \tag{2.5}$$

$$u_1(b,z) + b\frac{\partial}{\partial\rho}u_1(b,z) = 0 \quad , \quad z \in (-\infty,0) \tag{2.6}$$

$$u_2(d,z) + d\frac{\partial}{\partial\rho}u_2(d,z) = 0 \quad , \quad z \in (0,\infty) \tag{2.7}$$

$$\frac{\partial u_2(\rho,0)}{\partial z} = 0 \quad , \quad \rho \in (b,d) \tag{2.8}$$

which are derived from the fact that the tangential components of the electric field must be zero on the walls of the waveguide, and the continuity relations at $\rho = b$:

$$u_1(b,z) + b\frac{\partial}{\partial\rho}u_1(b,z) = u_2(b,z) + b\frac{\partial}{\partial\rho}u_2(b,z) \tag{2.9}$$

$$u_1(b,z) + \frac{e^{ikz}}{b} = u_2(b,z) \tag{2.10}$$

for $z \in (0,\infty)$, denoting that the tangential components of the electric fields and magnetic fields are continuous in the given region. Note that the incident field is a homogeneous solution of 2.4 satisfying boundary conditions 2.5 and 2.8. To ensure the uniqueness of the mixed boundary-value problem defined by the Helmholtz equation and the conditions 2.5-2.8, one has to take into account the radiation and edge conditions as well [16]. These statements are

$$\left(\frac{\partial u}{\partial r} - iku\right) = \mathcal{O}\left(r^{-1/2}\right), \quad r \to b \tag{2.11}$$

and

$$H_\phi = \mathcal{O}\left(z^{2/3}\right) \qquad E_z = \mathcal{O}\left(z^{-1/3}\right), \ z \to 0, \ \rho = b, d \tag{2.12}$$

respectively. The Fourier transform of the Helmholtz equation satisfied by $u_1(\rho,z)$ with respect to z, in the range of $z \in (-\infty,\infty)$ gives

$$\left[\frac{\partial^2}{\partial\rho^2} + \frac{1}{\rho}\frac{\partial}{\partial\rho} + \left(K^2(\alpha) - \frac{1}{\rho^2}\right)\right] F(\rho,\alpha) = 0 \tag{2.13}$$

Here

$$K(\alpha) = \sqrt{k^2 - \alpha^2} \tag{2.14}$$

is the square-root function defined in the complex α-plane, cut along $\alpha = k$ to $\alpha = k + i\infty$ and $\alpha = -k$ to $\alpha = -k - i\infty$, such that $K(0) = k$ as seen in Figure 2.2 and this choice of branch will be assumed for all square-root functions throughout the thesis.

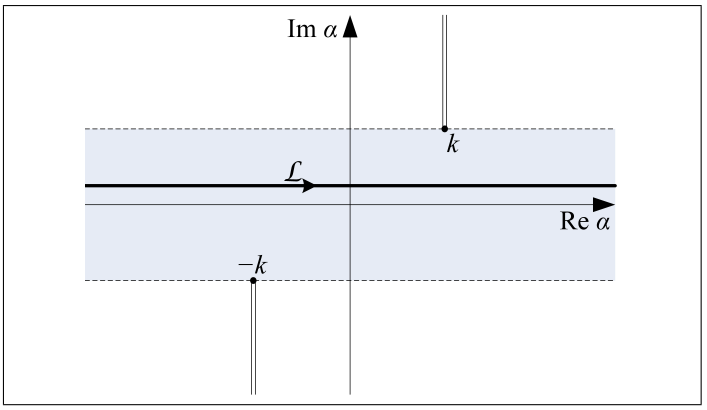

Figure 2.2: Complex α-plane.

The Fourier transform is defined by

$$F(\rho,\alpha) = F_{-}(\rho,\alpha) + F_{+}(\rho,\alpha) \tag{2.15}$$

where

$$F_{\pm}(\rho,\alpha) = \pm \int_{0}^{\pm\infty} u_1(\rho,z)\, e^{i\alpha z} dz. \tag{2.16}$$

Notice that $F_{+}(\rho,\alpha)$ and $F_{-}(\rho,\alpha)$ are unknown functions, which are regular in the half-planes $\mathrm{Im}(\alpha) > \mathrm{Im}(-k)$ and $\mathrm{Im}(\alpha) < \mathrm{Im}(k)$, respectively. The general solution of 2.13 is determined as described in [24]:

$$F(\rho,\alpha) = A(\alpha)\,\mathrm{J}_1(K\rho) + B(\alpha)\,\mathrm{Y}_1(K\rho) \tag{2.17}$$

Here $\mathrm{J}_1(K\rho)$ and $\mathrm{Y}_1(K\rho)$ are the usual Bessel functions of the first and second kinds, respectively. On the other hand, unknown $A(\alpha)$ and $B(\alpha)$ spectral coefficients are determined by use of the boundary conditions 2.5 and 2.6 which are satisfied on the perfect electric conductor (PEC) walls of the coaxial waveguide. First, applying the Fourier transform to the boundary condition 2.5 yields

$$\int_{-\infty}^{\infty} u_1(a,z)\, e^{i\alpha z} dz + a\frac{\partial}{\partial\rho}\int_{-\infty}^{\infty} u_1(a,z)\, e^{i\alpha z} dz = 0 \tag{2.18}$$

$$F(a,\alpha)+aF'(a,\alpha)=0 \tag{2.19}$$

where the prime denotes the first-order derivative with respect to ρ. Substituting 2.17 into 2.19:

$$\begin{aligned}&A(\alpha)\,\mathrm{J}_1(Ka)+B(\alpha)\,\mathrm{Y}_1(Ka)\\&\quad+a\{A(\alpha Ka)-\frac{1}{Ka}\mathrm{J}_1(Ka)]+B(\alpha)K[\mathrm{Y}_0(Ka)-\frac{1}{Ka}\mathrm{Y}_1(Ka)]\}=0\end{aligned} \tag{2.20}$$

$$A(\alpha)\,\mathrm{J}_0(Ka)+B(\alpha)\,\mathrm{Y}_0(Ka)=0 \tag{2.21}$$

$$B(\alpha)=-A(\alpha)\frac{\mathrm{J}_0(Ka)}{\mathrm{Y}_0(Ka)} \tag{2.22}$$

Substituting 2.22 into 2.17, one gets the following equation.

$$F(\rho,\alpha)=\frac{A(\alpha)}{\mathrm{Y}_0(Ka)}\left[\mathrm{J}_1(K\rho)\,\mathrm{Y}_0(Ka)-\mathrm{J}_0(Ka)\,\mathrm{Y}_1(K\rho)\right] \tag{2.23}$$

Secondly, applying the Fourier transform to the boundary condition 2.6 yields

$$\int_{-\infty}^{0}u_1(b,z)\,e^{i\alpha z}dz+b\frac{\partial}{\partial\rho}\int_{-\infty}^{0}u_1(b,z)\,e^{i\alpha z}dz=0 \tag{2.24}$$

$$F_-(b,\alpha)+bF'_-(b,\alpha)=0 \tag{2.25}$$

On the other hand, it can be written that

$$F(b,\alpha)+bF'(b,\alpha)=F_-(b,\alpha)+bF'_-(b,\alpha)+F_+(b,\alpha)+bF'_+(b,\alpha) \tag{2.26}$$

Substituting 2.25 into 2.26, one can obtain the following statement:

$$F(b,\alpha)+bF'(b,\alpha)=F_{+}(b,\alpha)+bF'_{+}(b,\alpha) \tag{2.27}$$

In addition, substituting 2.23 into 2.27 for $\rho=b$ yields

$$A(\alpha)=\frac{\left[F_{+}(b,\alpha)+bF'_{+}(b,\alpha)\right]\mathrm{Y}_0(Ka)}{Kb\left[\mathrm{J}_0(Kb)\,\mathrm{Y}_0(Ka)-\mathrm{J}_0(Ka)\,\mathrm{Y}_0(Kb)\right]} \tag{2.28}$$

Hence, equation 2.23 becomes

$$F(\rho,\alpha)=P_{+}(\alpha)\,\frac{\left[\mathrm{J}_1(K\rho)\,\mathrm{Y}_0(Ka)-\mathrm{J}_0(Ka)\,\mathrm{Y}_1(K\rho)\right]}{Kb\left[\mathrm{J}_0(Kb)\,\mathrm{Y}_0(Ka)-\mathrm{J}_0(Ka)\,\mathrm{Y}_0(Kb)\right]} \tag{2.29}$$

where $P_{+}(\alpha)$ stands for

$$P_{+}(\alpha)=F_{+}(b,\alpha)+bF'_{+}(b,\alpha) \tag{2.30}$$

Similarly, the scattered field $u_2(\rho,z)$ satisfies the Helmholtz equation, in the region described by $\rho\in(b,d)$, $z\in(0,\infty)$, whose Fourier transform with respect to z yields

$$\left[\frac{\partial^2}{\partial\rho^2}+\frac{1}{\rho}\frac{\partial}{\partial\rho}+\left(K^2(\alpha)-\frac{1}{\rho^2}\right)\right]G_{+}(\rho,\alpha)=-i\alpha f(\rho) \tag{2.31}$$

where the boundary condition 2.8 is taken into account. $G_{+}(\rho,\alpha)$, which is regular in the half-plane $\mathrm{Im}(\alpha)>\mathrm{Im}(-k)$, and $f(\rho)$ stands for

$$G_{+}(\rho,\alpha)=\int_0^{\infty}u_2(r,z)\,e^{i\alpha z}d\alpha \tag{2.32}$$

and

$$f(\rho)=u_2(\rho,0) \tag{2.33}$$

respectively. The general solution of this nonhomogeneous differential equation is the

sum of a particular solution of the nonhomogeneous equation and the general solution of the related homogeneous equation.

$$G_+(\rho,\alpha) = G_+^p(\rho,\alpha) + G_+^h(\rho,\alpha) \tag{2.34}$$

In equation 2.34 $G_+^p(\rho,\alpha)$ and $G_+^h(\rho,\alpha)$ represent the particular and homogeneous solutions, respectively. A particular solution of 2.31 can be expressed in terms of

$$G_+^p(\rho,\alpha) = -i\alpha \int_b^d f(t)\mathcal{G}(t,\rho,\alpha)\, tdt \tag{2.35}$$

following the procedure described in [25]. In equation 2.35, $\mathcal{G}(\rho,t,\alpha)$ is the Green's function related to this differential equation and it satisfies the Helmholtz equation.

$$\left[\frac{1}{\rho}\frac{\partial}{\partial\rho}\left(\rho\frac{\partial}{\partial\rho}\right) + \left(K^2(\alpha) - \frac{1}{\rho^2}\right)\right]\mathcal{G}(\rho,t,\alpha) = \frac{\delta(\rho-t)}{t} \tag{2.36}$$

for $\rho, t \in (b,d)$ with the associated continuity relations and boundary conditions which are given as follows.

$$\mathcal{G}(t+0,t,\alpha) - \mathcal{G}(t-0,t,\alpha) = 0 \tag{2.37}$$

$$\frac{\partial}{\partial\rho}\mathcal{G}(t+0,t,\alpha) - \frac{\partial}{\partial\rho}\mathcal{G}(t-0,t,\alpha) = \frac{1}{t} \tag{2.38}$$

$$\mathcal{G}(b,t,\alpha) + b\frac{\partial}{\partial\rho}\mathcal{G}(b,t,\alpha) = 0 \tag{2.39}$$

$$\mathcal{G}(d,t,\alpha) + d\frac{\partial}{\partial\rho}\mathcal{G}(d,t,\alpha) = 0 \tag{2.40}$$

Note that the continuity relations 2.37 and 2.38 are written in the region described by $\rho \in (b,d), z \in (0,\infty)$.

The general solution of this Green's function in 2.36 is in the form of

$$\mathcal{G}(\rho,t,\alpha)=\begin{cases} A(\alpha)\,\mathrm{J}_1(K\rho)+B(\alpha)\,\mathrm{Y}_1(K\rho) & , \quad b<\rho<t \\ C(\alpha)\,\mathrm{J}_1(K\rho)+D(\alpha)\,\mathrm{Y}_1(K\rho) & , \quad t<\rho<d \end{cases} \tag{2.41}$$

where $A(\alpha)$, $B(\alpha)$, $C(\alpha)$ and $D(\alpha)$ are the unknown spectral coefficients. Taking into account the conditions given in 2.37-2.40, the Green's function is determined as

$$\mathcal{G}(\rho,t,\alpha)=\frac{\mathcal{Q}(\rho,t,\alpha)}{M(b,d,\alpha)} \tag{2.42}$$

with

$$\mathcal{Q}(\rho,t,\alpha)=\frac{\pi}{2}\begin{cases} L(t,d,\alpha)\,L(\rho,b,\alpha) & , \quad b<\rho<t \\ L(t,b,\alpha)\,L(\rho,d,\alpha) & , \quad t<\rho<d \end{cases} \tag{2.43}$$

and

$$M(\rho_1,\rho_2,\alpha)=\mathrm{J}_0(K\rho_1)\,\mathrm{Y}_0(K\rho_2)-\mathrm{J}_0(K\rho_2)\,\mathrm{Y}_0(K\rho_1) \tag{2.44}$$

In 2.43, $L(\rho_1,\rho_2,\alpha)$ stands for

$$L(\rho_1,\rho_2,\alpha)=\mathrm{J}_1(K\rho_1)\,\mathrm{Y}_0(K\rho_2)-\mathrm{J}_0(K\rho_2)\,\mathrm{Y}_1(K\rho_1) \tag{2.45}$$

Substituting 2.42 into 2.35 allows one to get a particular solution.

$$G_+^p(\rho,\alpha)=-\frac{1}{M(b,d,\alpha)}(i\alpha)\int_b^d f(t)\,\mathcal{Q}(t,\rho,\alpha)\,tdt \tag{2.46}$$

On the other hand, the homogeneous solution $G_+^h(\rho,\alpha)$ is determined as the following statement.

$$G_+^h(\rho,\alpha)=C(\alpha)\,\mathrm{J}_1(K\rho)+D(\alpha)\,\mathrm{Y}_1(K\rho) \tag{2.47}$$

where $C(\alpha)$ and $D(\alpha)$ are the unknown spectral coefficients. The Fourier transform of the boundary condition 2.7 yields

$$G_+^h(\rho,\alpha) = \frac{C(\alpha)}{\mathrm{Y}_0(Kd)}[\mathrm{J}_1(K\rho)\,\mathrm{Y}_0(Kd) - \mathrm{J}_0(Kd)\,\mathrm{Y}_1(K\rho)] \tag{2.48}$$

As mentioned before, the general solution $G_+(\rho,\alpha)$ is the sum of a particular solution $G_+^p(\rho,\alpha)$ and the homogeneous solution $G_+^h(\rho,\alpha)$. Therefore,

$$G_+(\rho,\alpha) = \frac{C(\alpha)}{\mathrm{Y}_0(Kd)}[\mathrm{J}_1(K\rho)\,\mathrm{Y}_0(Kd) - \mathrm{J}_0(Kd)\,\mathrm{Y}_1(K\rho)] - \frac{1}{M(b,d,\alpha)}(i\alpha)\int_b^d f(t)\,\mathcal{Q}(t,\rho,\alpha)\,tdt \tag{2.49}$$

For the sake of the analytical convenience, $\tilde{C}(\alpha)$ coefficient can be defined as follows:

$$\tilde{C}(\alpha) = \frac{C(\alpha)\,M(b,d,\alpha)}{\mathrm{Y}_0(Kd)} \tag{2.50}$$

Rearranging 2.49 yields

$$G_+(\rho,\alpha) = \frac{1}{M(b,d,\alpha)}\left\{\tilde{C}(\alpha)\,[\mathrm{J}_1(K\rho)\,\mathrm{Y}_0(Kd) - \mathrm{J}_0(Kd)\,\mathrm{Y}_1(K\rho)] - i\alpha\int_b^d f(t)\,\mathcal{Q}(t,\rho,\alpha)\,tdt\right\} \tag{2.51}$$

The Fourier transform of the continuity relation 2.9 allows one to write,

$$F_+(b,\alpha) + bF_+'(b,\alpha) = G_+(b,\alpha) + bG_+'(b,\alpha) \tag{2.52}$$

Substituting 2.51 into 2.52 yields

$$\tilde{C}(\alpha) = \frac{P_+(\alpha)}{Kb} \tag{2.53}$$

Note that $P_+(\alpha)$ in 2.53 equals:

$$P_+(\alpha) = F_+(b,\alpha) + bF'_+(b,\alpha) \tag{2.54}$$

and 2.51 becomes

$$G_+(\rho,\alpha) = \frac{1}{K^2 bM(b,d,\alpha)} \{P_+(\alpha) K [\mathrm{J}_1(K\rho)\,\mathrm{Y}_0(Kd) - \mathrm{J}_0(Kd)\,\mathrm{Y}_1(K\rho)] - i\alpha b \int_b^d f(t) K^2 \mathcal{Q}(t,\rho,\alpha)\, tdt\Big\} \tag{2.55}$$

Although the left-hand side of 2.55 at $\rho = b$ is a regular function of in the upper half-plane, the regularity of the right-hand side is violated by the presence of simple poles occurring at the zeros of $K^2 M(b,d,\alpha)$ lying in the upper half of the complex $\alpha-$plane, namely, at $\alpha = \gamma_m$'s $(m = 0,1,2,...)$. These poles can be eliminated by imposing that their residues are zero. This gives

$$\Big[P_+(\alpha) K [\mathrm{J}_1(K\rho)\,\mathrm{Y}_0(Kd) - \mathrm{J}_0(Kd)\,\mathrm{Y}_1(K\rho)] - i\alpha b \int_b^d f(t) K^2 \mathcal{Q}(t,\rho,\alpha)\, tdt\Big]_{\rho=b,\alpha=\gamma_m} = 0 \tag{2.56}$$

becomes,

$$P_+(\Gamma_m)\Gamma_m [\mathrm{J}_1(\Gamma_m b)\,\mathrm{Y}_0(\Gamma_m d) - \mathrm{J}_0(\Gamma_m d)\,\mathrm{Y}_1(\Gamma_m b)] = i\gamma_m b \int_b^d f(t)\Gamma_m^2 \mathcal{Q}(t,b,\gamma_m)\, tdt \tag{2.57}$$

where

$$\mathcal{Q}(t,b,\gamma_m) = \frac{\pi}{2} L(b,b,\gamma_m) L(t,d,\gamma_m) \quad , \ \rho = b \tag{2.58}$$

The function $L(b,b,\gamma_m)$ in 2.57 can be written in terms of its Wronskian as in 2.59.

$$L(b,b,\gamma_m) = \mathrm{J}_1(\Gamma_m b)\,\mathrm{Y}_0(\Gamma_m b) - \mathrm{J}_0(\Gamma_m b)\,\mathrm{Y}_1(\Gamma_m b) = \frac{2}{\pi\Gamma_m b} \tag{2.59}$$

Substituting 2.58 and 2.59 into 2.57 yields

$$P_+(\gamma_m)\frac{\pi\Gamma_m}{2i\gamma_m}\left[\mathrm{J}_1(\Gamma_m b)\,\mathrm{Y}_0(\Gamma_m d) - \mathrm{J}_0(\Gamma_m d)\,\mathrm{Y}_1(\Gamma_m b)\right] = \int_b^d f(t)\,\frac{\pi}{2}\Gamma_m L(t,d,\gamma_m)\,tdt \tag{2.60}$$

Since $f(t)$ is a absolutely integrable function which satisfies the Dini's criterion, it can be expanded into the Fourier-Bessel series as follows:

$$f(t) = \sum_{m=0}^{\infty} f_m \varphi_m \tag{2.61}$$

with

$$\varphi_m = \frac{\pi}{2}\Gamma_m L(t,d,\gamma_m) \quad , \; m = 1,2,\ldots \tag{2.62}$$

where f_m and φ_m are the normalized Bessel coefficients and the related set of orthogonal functions, respectively. This series expansion allows one to write

$$f_m = \frac{1}{v_m^2}\int_b^d f(t)\,\frac{\pi}{2}\Gamma_m L(t,d,\gamma_m)\,tdt \tag{2.63}$$

in which v_m^2 is the norm of the related series expansion determined by making use of the orthogonality integral given by:

$$v_m^2 = \int_b^d \frac{\pi}{2} K L(t,d,\alpha)\,\frac{\pi}{2}\Gamma_m L(t,d,\gamma_m)\,tdt\Big|_{\alpha=\gamma_m} \tag{2.64}$$

Equation 2.64 is evaluated as:

$$v_m^2 = \frac{\mathrm{Y}_0^2(\Gamma_m b) - \mathrm{Y}_0^2(\Gamma_m d)}{2\mathrm{Y}_0^2(\Gamma_m b)} \tag{2.65}$$

On the other hand, rearranging 2.60 according to 2.63 yields

$$v_m^2 f_m = P_+(\gamma_m)\frac{\pi\Gamma_m}{2i\gamma_m}\left[\mathrm{J}_1(\Gamma_m b)\,\mathrm{Y}_0(\Gamma_m d) - \mathrm{J}_0(\Gamma_m d)\,\mathrm{Y}_1(\Gamma_m b)\right] \tag{2.66}$$

Note that f_m Bessel coefficients are determined by substituting 2.65 into 2.66.

$$f_m = \frac{2}{i\gamma_m b}\frac{\mathrm{Y}_0(\Gamma_m d)\,\mathrm{Y}_0(\Gamma_m b)}{\left[\mathrm{Y}_0^2(\Gamma_m b) - \mathrm{Y}_0^2(\Gamma_m d)\right]}P_+(\gamma_m) \quad , \; m = 1, 2, ... \tag{2.67}$$

and

$$f_0 = \frac{P_+(k)}{ikb\log(d/b)} \tag{2.68}$$

with f_m given by 2.63 and

$$f_0 = \frac{1}{\log(d/b)}\int_b^d f(t)\,dt \tag{2.69}$$

As mentioned before, $f(\rho)$ can be represented as its Fourier-Bessel series. Owing to 2.67-2.69,

$$f(\rho) = \frac{f_0}{\rho} + \sum_{m=1}^{\infty} f_m\left\{\frac{\pi}{2}\Gamma_m L(\rho, d, \gamma_m)\right\} \tag{2.70}$$

$$f(\rho) = \frac{f_0}{\rho} + \sum_{m=1}^{\infty} f_m\left\{\frac{\pi}{2}\Gamma_m\left[\mathrm{J}_1(\Gamma_m\rho)\,\mathrm{Y}_0(\Gamma_m d) - \mathrm{J}_0(\Gamma_m d)\,\mathrm{Y}_1(\Gamma_m\rho)\right]\right\} \tag{2.71}$$

The Fourier transform of the continuity relation 2.10 allows one to write

$$F_+(b, \alpha) - \frac{1}{ib(\alpha + k)} = G_+(b, \alpha) \tag{2.72}$$

Substituting 2.55 into 2.69 yields

$$P_+(\alpha)\frac{K\left[\mathrm{J}_1(Kb)\,\mathrm{Y}_0(Kd)-\mathrm{J}_0(Kd)\,\mathrm{Y}_1(Kb)\right]}{K^2bM(b,d,\alpha)} - \frac{i\alpha b}{K^2bM(b,d,\alpha)}\int_b^d f(t)\,K^2\mathcal{Q}(t,b,\alpha)\,tdt = F_+(b,\alpha) \quad (2.73)$$

Making use of 2.15 and 2.29, 2.70 can be written as follows:

$$\frac{P_+(\alpha)}{K^2}\left[\frac{K\mathrm{J}_1(Kb)\,\mathrm{Y}_0(Kd)-\mathrm{J}_0(Kd)\,\mathrm{Y}_1(Kb)}{\mathrm{J}_0(Kb)\,\mathrm{Y}_0(Kd)-\mathrm{J}_0(Kd)\,\mathrm{Y}_0(Kb)} + \frac{K\mathrm{J}_1(Kb)\,\mathrm{Y}_0(Ka)-\mathrm{J}_0(Ka)\,\mathrm{Y}_1(Kb)}{\mathrm{J}_0(Ka)\,\mathrm{Y}_0(Kb)-\mathrm{J}_0(Kb)\,\mathrm{Y}_0(Ka)}\right] + bF_-(b,\alpha) = \frac{i}{(\alpha+k)} + \frac{i\alpha b}{M(b,d,\alpha)}\int_b^d f(t)\,K^2\mathcal{Q}(t,b,\alpha)\,tdt \quad (2.74)$$

and then,

$$\frac{N(\alpha)}{(k^2-\alpha^2)}P_+(\alpha) + bP_-(\alpha) = \frac{i}{(\alpha+k)} + \frac{i\alpha b}{M(b,d,\alpha)}\int_b^d f(t)\,\mathcal{Q}(t,b,\alpha)\,tdt \quad (2.75)$$

with

$$N(\alpha) = \frac{2}{\pi b}\frac{M(a,d,\alpha)}{M(b,d,\alpha)\,M(a,b,\alpha)} \quad (2.76)$$

and

$$P_-(\alpha) = F_-(b,\alpha) \quad (2.77)$$

On the other hand, by use of 2.71, the last term of the right hand side of 2.75 is evaluated as follows:

$$\mathrm{I} = \int_b^d f(t)\,\mathcal{Q}(t,b,\alpha)\,tdt = \frac{M(b,d,\alpha)}{Kb}\left[\frac{f_0}{K} - K\sum_{m=1}^{\infty}\frac{f_m}{(\alpha^2-\gamma_m^2)}\frac{\mathrm{Y}_0(\Gamma_m d)}{\mathrm{Y}_0(\Gamma_m b)}\right] \quad (2.78)$$

Incorporating 2.78 into 2.75, we obtain

$$\frac{N(\alpha)}{(k^2-\alpha^2)}P_+(\alpha)+bF_-(b,\alpha)=\frac{i}{(\alpha+k)}+\frac{i\alpha f_0}{(k^2-\alpha^2)}-i\sum_{m=1}^{\infty}\frac{\alpha f_m}{(\alpha^2-\gamma_m^2)}\frac{\mathrm{Y}_0(\Gamma_m d)}{\mathrm{Y}_0(\Gamma_m b)} \tag{2.79}$$

Equation 2.79 is nothing but the modified Wiener-Hopf equation of the second type to be solved. Note that $N(\alpha)$ is the kernel function of the Wiener-Hopf equation which characterizes the nature of the step discontinuity on the outer wall of a coaxial waveguide.

2.1.2. The solution of MWHE

According to the classical Wiener-Hopf procedure, the kernel function $N(\alpha)$ is factorized into $N_+(\alpha)$ and $N_-(\alpha)$ as follows:

$$N(\alpha)=N_+(\alpha)N_-(\alpha) \tag{2.80}$$

in which $N_+(\alpha)$ and $N_-(\alpha)$ are regular and nonzero usual split functions in the half-planes $\mathrm{Im}(\alpha)>\mathrm{Im}(-k)$ and $\mathrm{Im}(\alpha)<\mathrm{Im}(k)$, respectively. Following the procedure, $N_\pm(\alpha)$ are to be as

$$N_\pm(\alpha)=\sqrt{\frac{2}{\pi b}}\frac{M_\pm(a,d,\alpha)}{M_\pm(b,d,\alpha)M_\pm(a,b,\alpha)} \tag{2.81}$$

where $M_\pm(\rho_1,\rho_2,\alpha)$ stands for the factorization of $M(\rho_1,\rho_2,\alpha)$ which is done by following the procedure described in [26]. Then, equation 2.79 becomes

$$\frac{N_+(\alpha)}{(k+\alpha)}P_+(\alpha)+\frac{(k-\alpha)}{N_-(\alpha)}bF_-(b,\alpha)=\frac{i}{(k+\alpha)}\frac{(k-\alpha)}{N_-(\alpha)}+\frac{i\alpha f_0}{(k+\alpha)}\frac{1}{N_-(\alpha)} -i\sum_{m=1}^{\infty}\frac{\alpha f_m}{(\alpha^2-\gamma_m^2)}\frac{\mathrm{Y}_0(\Gamma_m d)}{\mathrm{Y}_0(\Gamma_m b)}\frac{(k-\alpha)}{N_-(\alpha)} \tag{2.82}$$

Determining of unknown $P_{\pm}(\alpha)$ (note that $P_{-}(\alpha) = F_{-}(\alpha)$) requires that the function in the right hand side of 2.82 should be represented in the form of the sum of two regular functions on regions B_{+} and B_{-}. Note that B_{+} and B_{-} demonstrate the regions described by $\mathrm{Im}(\alpha) > \mathrm{Im}(-k)$ and $\mathrm{Im}(\alpha) < \mathrm{Im}(k)$, respectively. To remove the singularities in the right hand side of 2.82, the decomposition procedure is applied to the related equation by use of the Cauchy Residues Theorem.

$$\begin{aligned}\frac{N_{+}(\alpha)}{(k+\alpha)}P_{+}(\alpha) + \frac{(k-\alpha)}{N_{-}(\alpha)}bF_{-}(b,\alpha) &= \pm\frac{1}{2\pi i}\int_{L_{\pm}}\frac{i}{(k+\tau)}\frac{(k-\tau)}{N_{-}(\tau)}\frac{1}{\tau-\alpha}d\tau \\ &\pm\frac{1}{2\pi i}\int_{L_{\pm}}\frac{i\tau f_0}{(k+\tau)}\frac{1}{N_{-}(\tau)}\frac{1}{\tau-\alpha}d\tau \\ &\pm\frac{1}{2\pi i}\int_{L_{\pm}} i\sum_{m=1}^{\infty}\frac{-\tau f_m}{(\tau^2-\gamma_m^2)}\frac{\mathrm{Y}_0(\Gamma_m d)}{\mathrm{Y}_0(\Gamma_m b)}\frac{(k-\tau)}{N_{-}(\tau)}\frac{1}{\tau-\alpha}d\tau \quad (2.83)\end{aligned}$$

Following the integration, 2.83 becomes,

$$\begin{aligned}&\frac{N_{+}(\alpha)}{(k+\alpha)}P_{+}(\alpha) - \frac{i}{(k+\alpha)}\frac{2k}{N_{+}(k)} + \frac{if_0}{(k+\alpha)}\frac{k}{N_{+}(k)} \\ &+ i\sum_{m=1}^{\infty}\frac{f_m}{(\alpha+\gamma_m)}\frac{\mathrm{Y}_0(\Gamma_m d)}{\mathrm{Y}_0(\Gamma_m b)}\frac{(k+\gamma_m)}{2N_{+}(\gamma_m)} = \frac{if_0}{(k+\alpha)}\left[\frac{\alpha}{N_{-}(\alpha)} + \frac{k}{N_{+}(k)}\right] \\ &- \frac{(k-\alpha)}{N_{-}(\alpha)}bF_{-}(b,\alpha) + \frac{i}{(k+\alpha)}\left[\frac{(k-\alpha)}{N_{-}(\alpha)} - \frac{2k}{N_{+}(k)}\right] \\ &- i\sum_{m=1}^{\infty}\frac{f_m}{(\alpha+\gamma_m)}\frac{\mathrm{Y}_0(\Gamma_m d)}{\mathrm{Y}_0(\Gamma_m b)}\left[\frac{\alpha(k-\alpha)}{(\alpha-\gamma_m)N_{-}(\alpha)} - \frac{(k+\gamma_m)}{2N_{+}(\gamma_m)}\right] \quad (2.84)\end{aligned}$$

The left hand side of 2.84 is the sum of terms which are regular on region B_{+}, while the right hand side is the sum of terms which are regular on region B_{-}. 2.84 can be separated to two different equations symbolized by $W_{+}(\alpha)$ and $W_{-}(\alpha)$.

$$\begin{aligned}W_{+}(\alpha) = &\frac{i}{(k+\alpha)}\frac{2k}{N_{+}(k)} - \frac{if_0}{(k+\alpha)}\frac{k}{N_{+}(k)} \\ &- i\sum_{m=1}^{\infty}\frac{f_m}{(\alpha+\gamma_m)}\frac{\mathrm{Y}_0(\Gamma_m d)}{\mathrm{Y}_0(\Gamma_m b)}\frac{(k+\gamma_m)}{2N_{+}(\gamma_m)} - \frac{N_{+}(\alpha)}{(k+\alpha)}P_{+}(\alpha) \\ &, \ \alpha \in B_{+} \quad (2.85)\end{aligned}$$

and

$$W_{-}(\alpha)=\frac{i}{(k+\alpha)}\left[\frac{(k-\alpha)}{N_{-}(\alpha)}-\frac{2k}{N_{+}(k)}\right]+\frac{if_0}{(k+\alpha)}\left[\frac{\alpha}{N_{-}(\alpha)}+\frac{k}{N_{+}(k)}\right]$$
$$-i\sum_{m=1}^{\infty}\frac{f_m}{(\alpha+\gamma_m)}\frac{\mathrm{Y}_0(\Gamma_m d)}{\mathrm{Y}_0(\Gamma_m b)}\left[\frac{\alpha(k-\alpha)}{(\alpha-\gamma_m)N_{-}(\alpha)}-\frac{(k+\gamma_m)}{2N_{+}(\gamma_m)}\right]$$
$$-\frac{(k-\alpha)}{N_{-}(\alpha)}bF_{-}(b,\alpha)\quad,\alpha\in B_{-}\qquad(2.86)$$

which each of them is regular (analytic) on the related domains.

At this point, the reader can clearly see that the equality of $W_{+}(\alpha)=W_{-}(\alpha)$ is valid on the intersection region B described by $B_{+}\cap B_{-}$. Then, it can be said that, $W_{+}(\alpha)$ is the analytical continuation of $W_{-}(\alpha)$ to domain B_{+}, and vice versa. Thus, it is possible to define an arbitrary entire function $W(\alpha)$ which is regular at all finite points of the entire α-complex plane as follows [27]:

$$W(\alpha)=\begin{cases}W_{+}(\alpha)\quad,\ \alpha\in B_{+}\\ W_{-}(\alpha)\quad,\ \alpha\in B_{-}\end{cases}\qquad(2.87)$$

In addition, it is required to evaluate the asymptotic behavior of the entire function $W(\alpha)$. In accordance with Liouville's theorem, $W(\alpha)$ is 0 for all α-values, since $W(\alpha)$ is asymptotically equivalent to 0 as $\alpha\rightarrow\infty$, and, it allows one to write $P_{+}(\alpha)$ as follows:

$$P_{+}(\alpha)=\frac{2ik}{N_{+}(\alpha)N_{+}(k)}-\frac{ikf_0}{N_{+}(\alpha)N_{+}(k)}$$
$$-\frac{i}{2}\sum_{m=1}^{\infty}\frac{f_m}{(\alpha+\gamma_m)}\frac{\mathrm{Y}_0(\Gamma_m d)}{\mathrm{Y}_0(\Gamma_m b)}\frac{(k+\alpha)(k+\gamma_m)}{N_{+}(\alpha)N_{+}(\gamma_m)}\qquad(2.88)$$

The unknown coefficients f_m ($m=0,1,2,...$) can be calculated by taking into account equations 2.67, 2.68 and 2.85 simultaneously, which yields the algebraic system of equations.

$$\frac{2k\chi_m}{N_+(k)}f_0 + f_m + (k+\gamma_m)\chi_m \sum_{n=1}^{\infty} \frac{f_n}{(\gamma_m+\gamma_n)} \frac{\mathrm{Y}_0(\Gamma_n d)}{\mathrm{Y}_0(\Gamma_n b)} \frac{(k+\gamma_n)}{N_+(\gamma_n)} = \frac{4k\chi_m}{N_+(k)} \tag{2.89}$$

for $m = 1, 2, ...$ This explicit statement can be written as,

$$\mathbf{Af} = \mathbf{B} \tag{2.90}$$

where the elements of $\mathbf{A}$, namely A_{mn} are

$$A_{00} = \left[N_+(k)\, b \log(d/b) + \frac{1}{N_+(k)} \right] \tag{2.91}$$

$$A_{m0} = \frac{2k\chi_m}{N_+(k)} \ , \ m = 1, 2, ... \tag{2.92}$$

$$A_{0n} = \frac{\mathrm{Y}_0(\Gamma_n d)}{N_+(\gamma_n)\,\mathrm{Y}_0(\Gamma_n b)} \ , \ n = 1, 2, ... \tag{2.93}$$

$$A_{mn} = \begin{cases} 1 + \chi_m \dfrac{\mathrm{Y}_0(\Gamma_m d)}{\mathrm{Y}_0(\Gamma_m b)} \dfrac{(k+\gamma_m)^2}{2\gamma_m N_+(\gamma_m)} & , \quad n = m \\ \dfrac{(k+\gamma_m)\chi_m}{(\gamma_m+\gamma_n)} \dfrac{\mathrm{Y}_0(\Gamma_n d)}{\mathrm{Y}_0(\Gamma_n b)} \dfrac{(k+\gamma_n)}{N_+(\gamma_n)} & , \quad n \neq m \end{cases} \quad , \ m, n = 1, 2, .. \tag{2.94}$$

and the elements of $\mathbf{B}$, namely B_m are

$$B_m = \begin{cases} \dfrac{2}{N_+(k)} & , \quad m = 0 \\ \dfrac{4k\chi_m}{N_+(k)} & , \quad m = 1, 2, ... \end{cases} \tag{2.95}$$

with

$$\chi_m = \frac{\mathrm{Y}_0(\Gamma_m d)\,\mathrm{Y}_0(\Gamma_m b)}{\left[\mathrm{Y}_0^2(\Gamma_m b) - \mathrm{Y}_0^2(\Gamma_m d)\right]} \frac{1}{\gamma_m b N_+(\gamma_m)} \tag{2.96}$$

for $m, n = 1, 2, ...$

2.1.3. Analysis of the scattered fields

The scattered field $u_1(\rho, z)$ can be determined by solving the inverse Fourier transform integral

$$u_1(\rho, z) = \frac{1}{2\pi} \int_{\mathcal{L}} F(\rho, \alpha) e^{-i\alpha z} d\alpha \tag{2.97}$$

Considering 2.29 and 2.88, the above integral becomes

$$\begin{aligned} u_1(\rho, z) = \frac{1}{2\pi} \int_{\mathcal{L}} \frac{2}{\pi b} \Bigg\{ & \frac{2k}{N_+(\alpha) N_+(k)} - \frac{k f_0}{N_+(\alpha) N_+(k)} \\ & - \frac{1}{2} \sum_{m=1}^{\infty} \frac{f_m}{(\alpha + \gamma_m)} \frac{\mathrm{Y}_0(\Gamma_m d)}{\mathrm{Y}_0(\Gamma_m b)} \frac{(k+\alpha)(k+\gamma_m)}{N_+(\alpha) N_+(\gamma_m)} \Bigg\} \\ & \times \frac{\pi K \left[\mathrm{J}_1(K\rho) \mathrm{Y}_0(2Ka) - \mathrm{J}_0(Ka) \mathrm{Y}_1(K\rho) \right]}{2(k^2 - \alpha^2) M(b, a, \alpha)} e^{-i\alpha z} d\alpha \end{aligned} \tag{2.98}$$

In order to determine the reflected field back to the region $z < 0$, the above integral can be evaluated by virtue of the application of the Cauchy Residues Theorem, yielding the sum of the residues related to the poles occurring at the simple zeros of $\left(k^2 - \alpha^2\right) M(b, a, \alpha)$ lying in the upper half-plane, namely, at $\alpha = \alpha_n$'s ($n = 0, 1, 2, ...$). In accordance with the law of residues, one can write the integral 2.98 as one on the closed contour consisted of the infinite upper semicircle arc C_R and the counter L_- as follows:

$$\int_{\mathcal{L}_-} \frac{2}{\pi b} F(\rho, \alpha) e^{-i\alpha z} d\alpha + \int_{\mathcal{C}_{\mathcal{R}}} \frac{2}{\pi b} F(\rho, \alpha) e^{-i\alpha z} d\alpha = 2\pi i \sum_{n=1}^{\infty} Rez(\alpha_n) \tag{2.99}$$

where $F(\rho, \alpha)$ is the integrand of 2.98. By making use of Jordan's lemma, it can be easily shown that C_R counter integral in equation 2.99 satisfies

$$\lim_{R\to\infty}\int_{\mathcal{C}_{\mathcal{R}}} F(\rho,\alpha)\, e^{-i\alpha z} d\alpha \to 0 \tag{2.100}$$

for

$$\lim_{\alpha\to\infty} F(\rho,\alpha) \to 0 \tag{2.101}$$

where $F(\rho,\alpha) = \mathcal{O}\left(\alpha^{-1/2}\right)$. Thus, the integral along the real axis is just the sum of complex residues in the contour as follows:

$$u_1(\rho,z) = \frac{1}{2\pi}\int_{\mathcal{L}_-} \frac{2}{\pi b} F(\rho,\alpha)\, e^{-i\alpha z} d\alpha = i\sum_{n=1}^{\infty} Rez(\alpha_n) \tag{2.102}$$

where the term $Rez(\alpha_n)$ represents the residues related to the poles. The right hand side of 2.99 is evaluated by:

$$\begin{aligned} i\sum_{n=1}^{\infty} Rez(\alpha_n) = \lim_{\alpha\to\alpha_n}(\alpha-\alpha_n)\, i\frac{2}{\pi b}\Bigg\{ & \frac{2k}{N_+(\alpha)N_+(k)} - \frac{kf_0}{N_+(\alpha)N_+(k)} \\ & -\frac{1}{2}\sum_{m=1}^{\infty}\frac{f_m}{(\alpha+\gamma_m)}\frac{\mathrm{Y}_0(\Gamma_m d)}{\mathrm{Y}_0(\Gamma_m b)}\frac{(k+\alpha)(k+\gamma_m)}{N_+(\alpha)N_+(\gamma_m)}\Bigg\} \\ & \times \frac{\pi K\left[\mathrm{J}_1(K\rho)\,\mathrm{Y}_0(Ka) - \mathrm{J}_0(Ka)\,\mathrm{Y}_1(K\rho)\right]}{2\left(k^2-\alpha^2\right)M(b,a,\alpha)} e^{-i\alpha z} \end{aligned} \tag{2.103}$$

and,

$$\begin{aligned} i\sum_{n=1}^{\infty} Rez(\alpha_n) = i\frac{2}{\pi b}\Bigg\{ & \frac{2k}{N_+(\alpha_n)N_+(k)} - \frac{kf_0}{N_+(\alpha_n)N_+(k)} \\ & -\frac{1}{2}\sum_{m=1}^{\infty}\frac{f_m}{(\alpha_n+\gamma_m)}\frac{\mathrm{Y}_0(\Gamma_m d)}{\mathrm{Y}_0(\Gamma_m b)}\frac{(k+\alpha_n)(k+\gamma_m)}{N_+(\alpha_n)N_+(\gamma_m)}\Bigg\} \\ & \times \frac{\pi K_n\left[\mathrm{J}_1(K\rho)\,\mathrm{Y}_0(Ka) - \mathrm{J}_0(Ka)\,\mathrm{Y}_1(K\rho)\right]}{2\left[\left(k^2-\alpha^2\right)M(b,a,\alpha)\right]'_{\alpha\to\alpha_n}} e^{-i\alpha_n z} \end{aligned} \tag{2.104}$$

Denoting the reflected field as

$$u_1(\rho,z) = R_0\frac{e^{-ikz}}{\rho} + \sum_{n=1}^{\infty} R_n \frac{\pi}{2} K_n \left[\mathrm{J}_1(K_n\rho)\,\mathrm{Y}_0(K_n a) - \mathrm{J}_0(K_n a)\,\mathrm{Y}_1(K_n\rho)\right] e^{-i\alpha_n z} \quad , \quad z<0 \tag{2.105}$$

with

$$K_n = \sqrt{k^2-\alpha_n^2} \tag{2.106}$$

By taking into account the equation 2.104, the reflection coefficient R_n is derived as follows:

$$R_n = \frac{2}{\pi b}\left\{\frac{kf_0}{N_+(\alpha_n)N_+(k)} - \frac{2k}{N_+(\alpha_n)N_+(k)} + \frac{1}{2}\sum_{m=1}^{\infty}\frac{f_m}{(\alpha_n+\gamma_m)}\frac{\mathrm{Y}_0(\Gamma_m d)}{\mathrm{Y}_0(\Gamma_m b)}\frac{(k+\alpha_n)(k+\gamma_m)}{N_+(\alpha_n)N_+(\gamma_m)}\right\} \times \frac{1}{\left[(k^2-\alpha^2)M(b,a,\alpha)\right]'_{\alpha\to\alpha_n}} \tag{2.107}$$

For the fundamental TEM mode reflected back to $z<0$, it is found

$$R_0 = \frac{1}{2b\log(b/a)N_+(k)N_+(k)}\left\{f_0 - 2 + N_+(k)\sum_{m=1}^{\infty}\frac{f_m}{N_+(\gamma_m)}\frac{\mathrm{Y}_0(\Gamma_m d)}{\mathrm{Y}_0(\Gamma_m b)}\right\} \tag{2.108}$$

In a similar fashion, the transmission coefficient can be determined by evaluating the integral in 2.98 for $z>0$. The transmitted field is

$$u_2(\rho,z) = T_0\frac{e^{-ikz}}{\rho} + \sum_{n=1}^{\infty} T_n \frac{\pi}{2} \xi_n \left[\mathrm{J}_1(\xi_n\rho)\,\mathrm{Y}_0(\xi_n a) - \mathrm{J}_0(\xi_n a)\,\mathrm{Y}_1(\xi_n\rho)\right] e^{i\beta_n z} \quad , \quad z>0 \tag{2.109}$$

with

$$\xi_n = \sqrt{k^2 - \beta_n^2} \tag{2.110}$$

and β_n's are the simple zeros of $\left(k^2 - \alpha^2\right) M(a,d,\alpha)$, where $\beta_0 = k$. The transmission coefficients T_n's and T_0 are derived as

$$T_n = -\left\{ \frac{2k}{N_+(k)} - \frac{kf_0}{N_+(k)} - \frac{1}{2}\sum_{m=1}^{\infty} \frac{f_m}{(\gamma_m - \beta_n)} \frac{\mathrm{Y}_0(\Gamma_m d)}{\mathrm{Y}_0(\Gamma_m b)} \frac{(k-\beta_n)(k+\gamma_m)}{N_+(\gamma_m)} \right\} \times \frac{M(b,d,\beta_n) N_+(\beta_n)}{\left[\left(k^2 - \alpha^2\right) M(a,d,\alpha)\right]'_{\alpha \to -\beta_n}} \tag{2.111}$$

and

$$T_0 = (f_0 - 2) \frac{\log(d/b)}{2\log(d/a)} \tag{2.112}$$

respectively.

2.2. Mode-Matching Analysis

The geometry of the problem is also suitable for applying the Mode-Matching technique[16]. For this type of formulation, the geometry is divided into two regions as shown in Figure 2.3, where region A is the part before the step discontinuity defined as $\rho \in (a,b), z < 0$ and region B is the part after the step discontinuity defined as $\rho \in (a,d), z > 0$. Let the incident TEM mode propagating in the positive z direction be given by

$$H_\phi^i(\rho,z) = u_i(\rho,z) = \frac{e^{ikz}}{\rho} \tag{2.113}$$

where k is the propagation constant. The $\phi-$component of the total magnetic field at each region is defined as

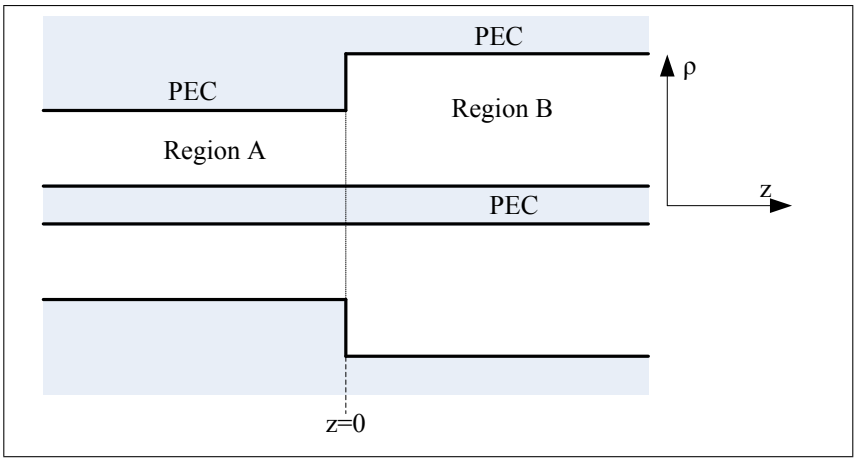

Figure 2.3: Regions for Mode-Matching technique.

$$H_{\phi}^{T}=\begin{cases}\dfrac{e^{ikz}}{\rho}+u_{1}\left(\rho,z\right) & ,\quad \rho\in\left(a,b\right),z<0\\ u_{2}\left(\rho,z\right) & ,\quad \rho\in\left(a,d\right),z>0\end{cases} \tag{2.114}$$

where $u_1(\rho,z)$ and $u_2(\rho,z)$ are the scattered fields in region A and region B, respectively. The geometry allows one to expand the field components in terms of their normal modes. Hence, the total field in region A can be written as

$$H_{\phi}^{A}\left(\rho,z\right)=\frac{\mathrm{e}^{\mathrm{i}kz}}{\rho}+u_{1}\left(\rho,z\right)=\frac{\mathrm{e}^{\mathrm{i}kz}}{\rho}+\sum_{n=0}^{\infty}R_{n}\varphi_{n}\left(\rho\right)e^{-i\alpha_{n}z} \tag{2.115}$$

where R_n is the reflection coefficient, $\varphi_n(\rho)$ is the eigenfunction and α_n is the wave number of the $n^{th.}$ modes of reflected wave, respectively. Similarly,

$$H_{\phi}^{B}\left(\rho,z\right)=u_{2}\left(\rho,z\right)=\sum_{n=0}^{\infty}T_{n}\psi_{n}\left(\rho\right)e^{i\beta_{n}z} \tag{2.116}$$

where T_n is the transmission coefficient of the $n^{th.}$ modes of transmitted wave and β_n's are the zeros of the function $\left(k^2-\alpha^2\right)M\left(d,a,\alpha\right)$ given by

$$\xi_{n}=\sqrt{k^{2}-\beta_{n}^{2}} \tag{2.117}$$

On the other hand, one can write $\rho-$component of the electric field as follows.

$$E_{\rho}^{A}(\rho,z)=\frac{1}{i\omega\epsilon}\frac{\partial}{\partial z}\left[\frac{\mathrm{e}^{\mathrm{i}kz}}{\rho}+u_1(\rho,z)\right]=\frac{k}{\omega\epsilon}\frac{\mathrm{e}^{\mathrm{i}kz}}{\rho}-\sum_{n=0}^{\infty}\frac{\alpha_n}{\omega\varepsilon}R_n\varphi_n(\rho)\,e^{-i\alpha_n z} \tag{2.118}$$

and

$$E_{\rho}^{B)}(\rho,z)=\frac{1}{i\omega\epsilon}\frac{\partial}{\partial z}u_2(\rho,z)=\sum_{n=0}^{\infty}\frac{\beta_n}{\omega\varepsilon}T_n\psi_n(\rho)\,e^{i\beta_n z} \tag{2.119}$$

The eigenfunctions $\varphi_n(\rho)$ and $\psi_n(\rho)$ in 2.118 and 2.119 stand for

$$\varphi_n(\rho)=\frac{\pi}{2}K_n\left[\mathrm{J}_1(K_n\rho)\,\mathrm{Y}_0(K_n a)-\mathrm{J}_0(K_n a)\,\mathrm{Y}_1(K_n\rho)\right] \tag{2.120}$$

and

$$\psi_n(\rho)=\frac{\pi}{2}\xi_n\left[\mathrm{J}_1(\xi_n\rho)\,\mathrm{Y}_0(\xi_n a)-\mathrm{J}_0(\xi_n a)\,\mathrm{Y}_1(\xi_n\rho)\right] \tag{2.121}$$

respectively, with K_n and ξ_n are being given by 2.106 and 2.117. Note that the eigenfunctions in the Fourier-Bessel series in 2.115 and 2.116 are determined, such that $u_1(\rho,z)$ and $u_2(\rho,z)$ are the solution of the Helmholtz equation, satisfying the boundary conditions given by:

$$u_1(a,z)+a\frac{\partial}{\partial\rho}u_1(a,z)=0 \tag{2.122}$$

$$u_1(b,z)+b\frac{\partial}{\partial\rho}u_1(b,z)=0 \tag{2.123}$$

$$u_2(a,z)+a\frac{\partial}{\partial\rho}u_2(a,z)=0 \tag{2.124}$$

$$u_2(d,z)+d\frac{\partial}{\partial\rho}u_2(d,z)=0 \tag{2.125}$$

In addition, $u_2(\rho, z)$ and its derivative are continuous at $z = 0$.

$$u_2(\rho, 0) = \begin{cases} 0 & , \quad \rho \in (a, b) \\ \dfrac{e^{ikz}}{\rho} + u_1(\rho, 0) & , \quad \rho \in (b, d) \end{cases} \tag{2.126}$$

The unknown coefficients R_n and T_n in the series expansions are determined by taking into account the continuity of the tangential components of the electric and the magnetic fields at $z = 0$, namely

$$E_\rho^B(\rho) = \begin{cases} E_\rho^A(\rho) & , \quad \rho \in (a, b) \\ 0 & , \quad \rho \in (b, d) \end{cases} \tag{2.127}$$

and

$$H_\phi^B(\rho) = H_\phi^B(\rho) \ , \quad \rho \in (a, b) \tag{2.128}$$

Substituting 2.118 and 2.119 into 2.127 yields

$$\sum_{n=0}^{\infty} \frac{\beta_n}{\omega\varepsilon} T_n \psi_n(\rho) = -\sum_{n=0}^{\infty} \frac{\alpha_n}{\omega\varepsilon} R_n \varphi_n(\rho) + \frac{k}{\omega\varepsilon}\frac{1}{\rho} \ , \quad \rho \in (a, b) \tag{2.129}$$

Multiplying 2.129 by $\omega\varepsilon\psi_m(\rho)$ and then integrating it along $\rho \in (a, d)$ yields

$$\int_a^d \sum_{n=0}^{\infty} \beta_n T_n \psi_n(\rho)\psi_m(\rho)\rho d\rho = -\int_a^d \sum_{n=0}^{\infty} \alpha_n R_n \varphi_n(\rho)\psi_m(\rho)\rho d\rho + \int_a^d \frac{k}{\rho}\psi_m(\rho)\rho d\rho \tag{2.130}$$

The series expansions in 2.130 exists if and only if the related eigenfunctions satisfy the orthogonality integral given below:

$$\int_a^d \psi_n(\rho)\psi_m(\rho)\rho d\rho = 0 \ , \quad m \neq n \tag{2.131}$$

Then, 2.130 can be written as,

$$\beta_m T_m Q_m^{(1)} = kU_m^{(1)} - \sum_{n=0}^{\infty} \alpha_n R_n \Delta_{mn}^{(1)} \tag{2.132}$$

with

$$\Delta_{mn}^{(1)} = \int_a^b \varphi_n(\rho)\, \psi_m(\rho)\, \rho d\rho \tag{2.133}$$

$$Q_m^{(1)} = \int_a^d \psi_m(\rho)\, \psi_n(\rho)\, \rho d\rho \tag{2.134}$$

$$U_m^{(1)} = \int_a^b \psi_m(\rho)\, d\rho \tag{2.135}$$

Similarly, after substituting 2.115 and 2.116 into 2.128, multiplying the related equation by $\omega\varepsilon\varphi_m(\rho)$ and integrating it along $\rho \in (a, d)$ yields

$$U_m^{(2)} + R_m Q_m^{(2)} = \sum_{n=0}^{\infty} T_n \Delta_{mn}^{(2)} \tag{2.136}$$

with

$$\Delta_{mn}^{(2)} = \int_a^b \varphi_m(\rho)\, \psi_n(\rho)\, \rho d\rho \tag{2.137}$$

$$Q_m^{(2)} = \int_a^b \varphi_n(\rho)\, \varphi_m(\rho)\, \rho d\rho \tag{2.138}$$

$$U_m^{(2)} = \int_a^b \varphi_m(\rho)\, d\rho \tag{2.139}$$

The reader notes that the set of equations in 2.132 is derived by matching the fields at z=0 and in the region A defined by $a < \rho < b$, while the set of equations in 2.136 is

a result of matching the fields at z=0 and in the region B defined by $a < \rho < d$. In this respect, the set of equations pair are regarded as a doubly infinite set of equations which must be solved simultaneously. As a result, the main equations are given by

$$\beta_m T_m Q_m^{(1)} = kU_m^{(1)} - \sum_{n=0}^{\infty} \alpha_n R_n \Delta_{mn}^{(1)} \ , \ m = 0, 1, 2, ..., \infty \tag{2.140}$$

and

$$U_m^{(2)} + R_m Q_m^{(2)} = \sum_{n=0}^{\infty} T_n \Delta_{mn}^{(2)} \ , \ m = 0, 1, 2, ..., \infty \tag{2.141}$$

The solution of this doubly infinite set of equations entails truncating the first and the second equations with a truncation number such P and Q, respectively.

$$\beta_m T_m Q_m^{(1)} = kU_m^{(1)} - \sum_{n=0}^{P} \alpha_n R_n \Delta_{mn}^{(1)} \ , \ m = 0, 1, 2, ..., P \tag{2.142}$$

and

$$U_m^{(2)} + R_m Q_m^{(2)} = \sum_{n=0}^{Q} T_n \Delta_{mn}^{(2)} \ , \ m = 0, 1, 2, ..., Q \tag{2.143}$$

This truncating procedure yields a $(N+2) \times (N+2)$ system with $N = P + Q$. Note that P must be greater than Q since the first set of equations involves more information than the latter. The explicit expressions for $\Delta_{mn}^{(1)}$, $\Delta_{mn}^{(2)}$, $Q_m^{(1)}$, $Q_m^{(2)}$, $U_m^{(1)}$ and $U_m^{(2)}$ are

$$\Delta_{mn}^{(1)} = \begin{cases} \log(b/a) & , \ m = 0, n = 0 \\ 0 & , \ m = 0, n \neq 0 \\ \dfrac{\pi}{2} M(a, b, \beta_m) & , \ m \neq 0, n = 0 \\ \dfrac{\pi}{2} \dfrac{\xi_m^2}{(\xi_m^2 - K_n^2)} \dfrac{\mathrm{Y}_0(K_n a)}{\mathrm{Y}_0(K_n b)} M(a, b, \beta_m) & , \ m \neq 0, n \neq 0 \end{cases} \tag{2.144}$$

$$\Delta_{mn}^{(2)} = \begin{cases} \log(b/a) & , \quad m=0, n=0 \\ \frac{\pi}{2} M(a,b,\beta_n) & , \quad m=0, n\neq 0 \\ 0 & , \quad m\neq 0, n=0 \\ \frac{\pi}{2}\frac{\xi_n^2}{\left(\xi_n^2 - K_m^2\right)}\frac{\mathrm{Y}_0(K_m a)}{\mathrm{Y}_0(K_m b)} M(a,b,\beta_n) & , \quad m\neq 0, n\neq 0 \end{cases} \tag{2.145}$$

$$Q_m^{(1)} = \begin{cases} \log(d/a) & , \quad m=0 \\ \frac{\left[\mathrm{Y}_0^2(\xi_m a) - \mathrm{Y}_0^2(\xi_m d)\right]}{2\mathrm{Y}_0^2(\xi_m d)} & , \quad m\neq 0 \end{cases} \tag{2.146}$$

$$Q_m^{(2)} = \begin{cases} \log(b/a) & , \quad m=0 \\ \frac{\left[\mathrm{Y}_0^2(\xi_m a) - \mathrm{Y}_0^2(\xi_m b)\right]}{2\mathrm{Y}_0^2(\xi_m b)} & , \quad m\neq 0 \end{cases} \tag{2.147}$$

$$U_m^{(1)} = \begin{cases} \log(b/a) & , \quad m=0 \\ \frac{\pi}{2} M(a,b,\beta_m) & , \quad m\neq 0 \end{cases} \tag{2.148}$$

and

$$U_m^{(2)} = \begin{cases} \log(b/a) & , \quad m=0 \\ 0 & , \quad m\neq 0 \end{cases} \tag{2.149}$$

respectively.

3. STEP DISCONTINUITY ON THE INNER WALL

3.1. Wiener-Hopf Analysis

3.1.1. Formulation of the problem

Consider a semi-infinite coaxial cylindrical waveguide whose inner and outer cylindrical walls are located at $\rho = a$ for $z \in (-\infty, 0)$ and $\rho = b$ for $z \in (-\infty, 0)$ is connected to another semi-infinite coaxial cylindrical waveguide whose inner and outer cylindrical walls are located at $\rho = d$ for $z \in (0, \infty)$ and $\rho = b$ for $z \in (0, \infty)$ as illustrated in Figure 3.1. Note that the step discontinuity on the inner wall occurs at the point $z = 0$ for $\rho \in (a, d)$.

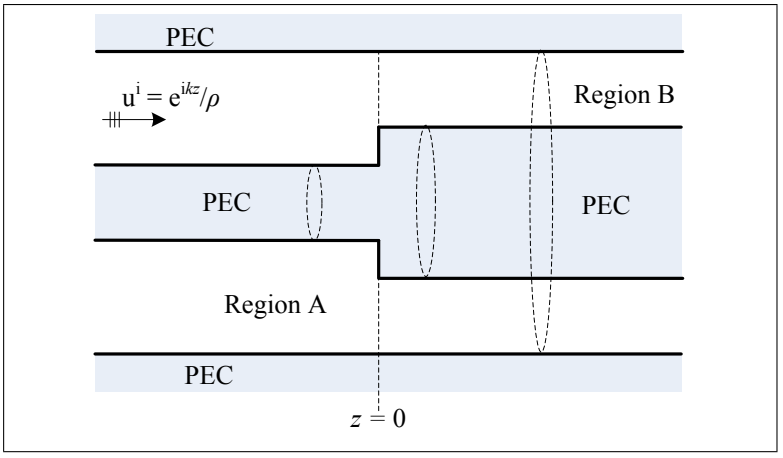

Figure 3.1: Geometry of the problem.

Let the incident TEM mode propagating in the positive z direction be given by

$$H_\phi^i(\rho, z) = u_i(\rho, z) = \frac{e^{ikz}}{\rho} \tag{3.1}$$

where k is the propagation constant which is assumed to have a small positive imaginary part corresponding to a slightly lossy medium. The lossless case can then be obtained by letting $\mathrm{Im}(k) \to 0$ at the end of the analysis. In virtue of the axial symmetry of the

problem, all the field components may be expressed in terms of $H_\phi(\rho,z) = u(\rho,z)$ as

$$E_\rho = \frac{1}{\mathrm{i}\omega\epsilon}\frac{\partial}{\partial z}u(\rho,z) \quad \text{and} \quad E_z = -\frac{1}{\mathrm{i}\omega\epsilon}\frac{1}{\rho}\frac{\partial}{\partial \rho}\left[\rho u(\rho,z)\right] \tag{3.2}$$

where the other components of the fields are zero. For the sake of analytical convenience, the total field $u_T(\rho,z)$ can be expressed as

$$u_T(\rho,z) = \begin{cases} u_i(\rho,z) + u_1(\rho,z) & , \quad d < \rho < b \\ \left[u_i(\rho,z) + u_2(\rho,z)\right]\mathrm{H}(-z) & , \quad a < \rho < d \end{cases} \tag{3.3}$$

with $\mathrm{H}(z)$ being the Heaviside step function and where $u_1(\rho,z)$ and $u_2(\rho,z)$ are the scattered fields which satisfy the Helmholtz equation

$$\left[\frac{\partial^2}{\partial\rho^2} + \frac{1}{\rho}\frac{\partial}{\partial\rho} + \frac{\partial^2}{\partial z^2} + \left(k^2 - \frac{1}{\rho^2}\right)\right] u_j(\rho,z) = 0 \quad , \quad j = 1,2 \tag{3.4}$$

in their domains of validity with the boundary conditions

$$u_1(b,z) + b\frac{\partial}{\partial\rho}u_1(b,z) = 0 \quad , \quad z \in (-\infty,\infty) \tag{3.5}$$

$$u_1(d,z) + d\frac{\partial}{\partial\rho}u_1(d,z) = 0 \quad , \quad z \in (0,\infty) \tag{3.6}$$

$$u_2(a,z) + a\frac{\partial}{\partial\rho}u_2(a,z) = 0 \quad , \quad z \in (-\infty,0) \tag{3.7}$$

$$\frac{\partial u_2(\rho,0)}{\partial z} = -\frac{\mathrm{i}k}{\rho} \quad , \quad \rho \in (a,d) \tag{3.8}$$

The continuity relations at $\rho = d$ are given by

$$u_1(d,z) + d\frac{\partial}{\partial\rho}u_1(d,z) = u_2(d,z) + d\frac{\partial}{\partial\rho}u_2(d,z) \quad , \quad z \in (-\infty,0) \tag{3.9}$$

and

$$u_1(d,z) = u_2(d,z) \quad , \quad z \in (-\infty, 0) \tag{3.10}$$

respectively. To ensure the uniqueness of the mixed boundary-value problem defined by the Helmholtz equation and the conditions 3.5-3.8, one has to take into account the radiation and edge conditions as well [16]. These statements are

$$\left(\frac{\partial u}{\partial r} - iku\right) = \mathcal{O}\left(r^{-1/2}\right), \quad r \to b \tag{3.11}$$

and

$$H_\phi = \mathcal{O}\left(z^{2/3}\right) \qquad E_z = \mathcal{O}\left(z^{-1/3}\right), \ z \to 0, \ \ \rho = a, d \tag{3.12}$$

The Fourier transform of the Helmholtz equation satisfied by $u_1(\rho, z)$ with respect to z in the range of $z \in (-\infty, \infty)$ gives

$$\left[\frac{\partial^2}{\partial \rho^2} + \frac{1}{\rho}\frac{\partial}{\partial \rho} + \left(K^2(\alpha) - \frac{1}{\rho^2}\right)\right] F(\rho, \alpha) = 0 \tag{3.13}$$

Here $K(\alpha) = \sqrt{k^2 - \alpha^2}$ is the square-root function defined in the complex α-plane, cut along $\alpha = k$ to $\alpha = k + \mathrm{i}\infty$ and $\alpha = -k$ to $\alpha = -k - \mathrm{i}\infty$, such that $K(0) = k$ and this choice of branch will be assumed for all square-root functions throughout the thesis as mentioned before. The Fourier transform is defined by

$$F(\rho, \alpha) = F_-(\rho, \alpha) + F_+(\rho, \alpha) \tag{3.14}$$

where

$$F_\pm(\rho, \alpha) = \pm \int_0^{\pm\infty} u_1(\rho, z)\, \mathrm{e}^{\mathrm{i}\alpha z} dz \tag{3.15}$$

Notice that $F_+(\rho,\alpha)$ and $F_-(\rho,\alpha)$ are unknown functions which are regular in the half-planes $\mathrm{Im}(\alpha) > \mathrm{Im}(-k)$ and $\mathrm{Im}(\alpha) < \mathrm{Im}(k)$, respectively. The general solution of 3.13 is determined as

$$F(\rho,\alpha) = A(\alpha)\,\mathrm{J}_1(K\rho) + B(\alpha)\,\mathrm{Y}_1(K\rho) \tag{3.16}$$

Here $\mathrm{J}_1(K\rho)$ and $\mathrm{Y}_1(K\rho)$ are the usual Bessel functions of the first and second kinds, respectively. As mentioned in chapter 2, one have to take into account the boundary conditions 3.5 and 3.8 to determine the unknown spectral coefficients $A(\alpha)$ and $B(\alpha)$. Applying the Fourier transform to the boundary condition 3.5 yields

$$B(\alpha) = -A(\alpha)\,\frac{\mathrm{J}_0(Kb)}{\mathrm{Y}_0(Kb)} \tag{3.17}$$

Substituting 3.17 into 3.16, one gets

$$F(\rho,\alpha) = \frac{A(\alpha)}{\mathrm{Y}_0(Kb)}\left[\mathrm{J}_1(K\rho)\,\mathrm{Y}_0(Kb) - \mathrm{J}_0(Kb)\,\mathrm{Y}_1(K\rho)\right] \tag{3.18}$$

Similarly, the Fourier transform of the boundary condition 3.6 gives

$$\int_0^\infty u_1(d,z)\,e^{i\alpha z}dz + d\frac{\partial}{\partial\rho}\int_0^\infty u_1(d,z)\,e^{i\alpha z}dz = 0 \tag{3.19}$$

$$F_+(d,\alpha) + dF'_+(d,\alpha) = 0 \tag{3.20}$$

where the prime denotes the first-order derivative with respect to ρ. On the other hand, it can be written that

$$F(d,\alpha) + dF'(d,\alpha) = F_-(d,\alpha) + dF'_-(d,\alpha) + F_+(d,\alpha) + dF'_+(d,\alpha) \tag{3.21}$$

Substituting 3.20 into 3.21 yields

$$F(b,\alpha)+bF'(b,\alpha)=F_{-}(b,\alpha)+bF'_{-}(b,\alpha) \tag{3.22}$$

Substituting 3.22 into 3.18, the spectral coefficient $A(\alpha)$ is written as:

$$A(\alpha)=\frac{\left[F_{-}(d,\alpha)+dF'_{-}(d,\alpha)\right]\mathrm{Y}_0(Kb)}{Kd\left[\mathrm{J}_0(Kd)\,\mathrm{Y}_0(Kb)-\mathrm{J}_0(Kb)\,\mathrm{Y}_0(Kd)\right]} \tag{3.23}$$

Hence, equation 3.18 becomes

$$F(\rho,\alpha)=P_{-}(\alpha)\frac{\left[\mathrm{J}_1(K\rho)\,\mathrm{Y}_0(Kb)-\mathrm{J}_0(Kb)\,\mathrm{Y}_1(K\rho)\right]}{Kd\left[\mathrm{J}_0(Kd)\,\mathrm{Y}_0(Kb)-\mathrm{J}_0(Kb)\,\mathrm{Y}_0(Kd)\right]} \tag{3.24}$$

where $P_{-}(\alpha)$ stands for

$$P_{-}(\alpha)=F_{-}(d,\alpha)+dF'_{-}(d,\alpha) \tag{3.25}$$

Similarly, the scattered field $u_2(\rho,z)$ satisfies the Helmholtz equation, in the region $\rho\in(a,d), z\in(-\infty,0)$, whose Fourier transform with respect to z yields

$$\left[\frac{\partial^2}{\partial\rho^2}+\frac{1}{\rho}\frac{\partial}{\partial\rho}+\left(K^2(\alpha)-\frac{1}{\rho^2}\right)\right]G_{-}(\rho,\alpha)=\mathrm{i}\alpha f(\rho)+\frac{\mathrm{i}k}{\rho} \tag{3.26}$$

where the boundary condition 3.8 is taken into account. $G_{-}(\rho,\alpha)$, which is regular in the half-plane $\mathrm{Im}(\alpha)<\mathrm{Im}(k)$, and $f(\rho)$ stand for

$$G_{-}(\rho,\alpha)=\int_{-\infty}^{0}u_2(\rho,z)\,\mathrm{e}^{\mathrm{i}\alpha z}dz \tag{3.27}$$

and

$$f(\rho)=u_2(\rho,0) \tag{3.28}$$

respectively. The general solution of this nonhomogeneous differential equation is

written by

$$G_{-}(\rho,\alpha) = G_{-}^{p}(\rho,\alpha) + G_{-}^{h}(\rho,\alpha) \tag{3.29}$$

where $G_{+}^{p}(\rho,\alpha)$ and $G_{+}^{h}(\rho,\alpha)$ represent the particular and homogeneous solutions, respectively. A particular solution of 3.26 can be expressed in terms of the Green's function related to this differential equation as follows:

$$G_{-}^{p}(\rho,\alpha) = i\alpha \int_{a}^{d} f(t)\mathcal{G}(\rho,t,\alpha)\, tdt + ik \int_{a}^{d} \mathcal{G}(\rho,t,\alpha)\, dt \tag{3.30}$$

where $\mathcal{G}(\rho,t,\alpha)$ is the Green's function satisfies the Helmholtz equation

$$\left[\frac{1}{\rho}\frac{\partial}{\partial\rho}\left(\rho\frac{\partial}{\partial\rho}\right) + \left(K^2(\alpha) - \frac{1}{\rho^2}\right)\right]\mathcal{G}(\rho,t,\alpha) = \frac{1}{t}\delta(\rho - t) \quad , \quad \rho,t \in (a,d) \tag{3.31}$$

where

$$\mathcal{G}(t+0,t,\alpha) - \mathcal{G}(t-0,t,\alpha) = 0 \tag{3.32}$$

and

$$\frac{\partial}{\partial\rho}\mathcal{G}(t+0,t,\alpha) - \frac{\partial}{\partial\rho}\mathcal{G}(t-0,t,\alpha) = \frac{1}{t} \tag{3.33}$$

with the boundary conditions

$$\mathcal{G}(a,t,\alpha) + a\frac{\partial}{\partial\rho}\mathcal{G}(a,t,\alpha) = 0 \tag{3.34}$$

and

$$\mathcal{G}(d,t,\alpha) + d\frac{\partial}{\partial\rho}\mathcal{G}(d,t,\alpha) = 0 \tag{3.35}$$

The general solution of this Green's function in 3.31 is in the form of

$$\mathcal{G}(\rho,t,\alpha)=\begin{cases} A(\alpha)\ \mathrm{J}_1(K\rho)+B(\alpha)\ \mathrm{Y}_1(K\rho) & ,\quad a<\rho<t \\ C(\alpha)\ \mathrm{J}_1(K\rho)+D(\alpha)\ \mathrm{Y}_1(K\rho) & ,\quad t<\rho<d \end{cases} \tag{3.36}$$

Taking into account the equations given in 3.5-3.8, the Green's function is determined as follows:

$$\mathcal{G}(\rho,t,\alpha)=\frac{\mathcal{Q}(\rho,t,\alpha)}{M(a,d,\alpha)} \tag{3.37}$$

In 3.37, $\mathcal{Q}(\rho,t,\alpha)$ is given by

$$\mathcal{Q}(\rho,t,\alpha)=\frac{\pi}{2}\begin{cases} L(t,d,\alpha)\,L(\rho,a,\alpha) & ,\quad a<\rho<t \\ L(t,a,\alpha)\,L(\rho,d,\alpha) & ,\quad t<\rho<d \end{cases} \tag{3.38}$$

where $M(\rho_1,\rho_2,\alpha)$ and $L(\rho_1,\rho_2,\alpha)$ are determined in 2.44 and 2.45, respectively. Substituting 3.37 into 3.30 allows one to get a particular solution.

$$G_{-}^{p}(\rho,\alpha)=\frac{1}{M(a,d,\alpha)}\left[i\alpha\int_a^d f(t)\mathcal{G}(\rho,t,\alpha)\,tdt+ik\int_a^d \mathcal{G}(\rho,t,\alpha)\,dt\right] \tag{3.39}$$

On the other hand, the homogeneous solution $G_{-}^{h}(\rho,\alpha)$ is determined as mentioned in chapter 2.

$$G_{-}^{h}(\rho,\alpha)=\frac{C(\alpha)}{\mathrm{Y}_0(Ka)}[\mathrm{J}_1(K\rho)\,\mathrm{Y}_0(Ka)-\mathrm{J}_0(Ka)\,\mathrm{Y}_1(K\rho)] \tag{3.40}$$

Hence, the general solution of 3.26 can be expressed as

$$\begin{aligned} G_{-}(\rho,\alpha)=\frac{1}{M(a,d,\alpha)}\Big\{&\tilde{C}(\alpha)\,[\mathrm{J}_1(K\rho)\,\mathrm{Y}_0(Ka)-\mathrm{J}_0(Ka)\,\mathrm{Y}_1(K\rho)] \\ &+\mathrm{i}\alpha\int_a^d f(t)\,\mathcal{Q}(t,\rho,\alpha)\,tdt+\mathrm{i}k\int_a^d \mathcal{Q}(t,\rho,\alpha)\,dt\Big\} \end{aligned} \tag{3.41}$$

Note that $\tilde{C}$ in equation 3.41 is given by

$$\tilde{C}(\alpha) = \frac{C(\alpha) M(a,d,\alpha)}{\mathrm{Y}_0(Ka)} \tag{3.42}$$

The Fourier transform of the continuity relation 3.9 allows one to write

$$F_-(d,\alpha) + dF'_-(d,\alpha) = G_-(d,\alpha) + dG'_-(d,\alpha) \tag{3.43}$$

Substituting 3.41 into 3.43, the unknown coefficient $\tilde{C}$ becomes

$$\tilde{C}(\alpha) = -\frac{P_-(\alpha)}{Kd} \tag{3.44}$$

where

$$P_-(\alpha) = F_-(d,\alpha) + dF'_-(d,\alpha) \tag{3.45}$$

Finally, equation 3.41 becomes

$$G_-(\rho,\alpha) = -\frac{1}{K^2 dM(a,d,\alpha)} \{P_-(\alpha) K [\mathrm{J}_1(K\rho)\mathrm{Y}_0(Ka) - \mathrm{J}_0(Ka)\mathrm{Y}_1(K\rho)] - \mathrm{i}\alpha \int_a^d f(t)\, \mathcal{Q}(t,\rho,\alpha)\, t dt - \mathrm{i}k \int_a^d \mathcal{Q}(t,\rho,\alpha)\, dt \Big\} \tag{3.46}$$

Although the left-hand side of 3.46 is a regular function of α in the lower half-plane, the regularity of the right-hand side is violated by the presence of simple poles occurring at the zeros of $K^2 M(a,d,\alpha)$ lying in the lower half of the complex $\alpha-$plane, namely, at $\alpha = -\gamma_m$'s ($m = 0, 1, 2, ...$). These poles can be eliminated by imposing that their residues are zero. This gives

$$\Big[P_{-}(\alpha) K\left[\mathrm{J}_1(K\rho)\,\mathrm{Y}_0(Ka)-\mathrm{J}_0(Ka)\,\mathrm{Y}_1(K\rho)\right] - \mathrm{i}\alpha\int_a^d f(t)\,\mathcal{Q}(t,\rho,\alpha)\,tdt - \mathrm{i}k\int_a^d \mathcal{Q}(t,\rho,\alpha)\,dt\Big]\Big|_{\rho=d,\alpha=-\gamma_m} \tag{3.47}$$

After the similar procedure given by 2.56-2.66, one can get

$$f_0 = 1 - \frac{P_{-}(-k)}{\mathrm{i}kd\log(d/a)} \tag{3.48}$$

and

$$f_m = -\frac{2\mathrm{Y}_0(\Gamma_m a)\,\mathrm{Y}_0(\Gamma_m d)}{\mathrm{i}\gamma_m d\left[\mathrm{Y}_0^2(\Gamma_m a)-\mathrm{Y}_0^2(\Gamma_m d)\right]} P_{-}(-\gamma_m) \tag{3.49}$$

with

$$f_0 = \frac{1}{\log(d/a)}\int_a^d f(t)\,dt, \tag{3.50}$$

$$f_m = \frac{2\mathrm{Y}_0^2(\Gamma_m d)}{\left[\mathrm{Y}_0^2(\Gamma_m a)-\mathrm{Y}_0^2(\Gamma_m d)\right]}\int_a^d f(t)\,\frac{\pi}{2}\Gamma_m L(t,a,\gamma_m)\,tdt \tag{3.51}$$

and

$$\Gamma_m = \sqrt{k^2-\gamma_m^2} \tag{3.52}$$

for $m = 1, 2, ...$ Owing to 3.48-3.51, $f(\rho)$ can be expanded into Fourier-Bessel series as

$$f(\rho) = \frac{f_0}{\rho} + \sum_{m=1}^{\infty} f_m\left\{\frac{\pi}{2}\Gamma_m\left[\mathrm{J}_1(\Gamma_m\rho)\,\mathrm{Y}_0(\Gamma_m a)-\mathrm{J}_0(\Gamma_m a)\,\mathrm{Y}_1(\Gamma_m\rho)\right]\right\} \tag{3.53}$$

Now, substituting 3.46 into the Fourier transform of the continuity relation 3.10 and making use of 3.14 and 3.24, one gets

$$\frac{N(\alpha)}{(k^2-\alpha^2)}P_-(\alpha) - dP_+(\alpha) = \frac{1}{(k^2-\alpha^2)M(a,d,\alpha)}\frac{2\mathrm{i}\alpha}{\pi}\int_a^d f(t)\left[\frac{\pi}{2}KL(t,a,\alpha)\right]tdt + \frac{\mathrm{i}k}{(k^2-\alpha^2)} \quad (3.54)$$

with

$$N(\alpha) = \frac{2}{\pi d}\frac{M(a,b,\alpha)}{M(a,d,\alpha)M(d,b,\alpha)} \quad (3.55)$$

and

$$P_+(\alpha) = F_+(d,\alpha) \quad (3.56)$$

Incorporating 3.53 into 3.54, one obtain after term by term integration

$$\frac{N(\alpha)}{(k^2-\alpha^2)}P_-(\alpha) - dP_+(\alpha) = \frac{\mathrm{i}(k+\alpha f_0)}{(k^2-\alpha^2)} - \mathrm{i}\sum_{m=1}^{\infty} f_m \frac{\alpha}{(\alpha^2-\gamma_m^2)}\frac{\Upsilon_0(\Gamma_m a)}{\Upsilon_0(\Gamma_m d)} \quad (3.57)$$

Equation 3.57 is nothing but the modified Wiener-Hopf equation of the second type to be solved. Note that $N(\alpha)$ is the kernel function of the Wiener-Hopf equation which characterizes the nature of the step discontinuity on the inner wall of a coaxial waveguide.

3.1.2. Solution of MWHE

Applying classical Wiener-Hopf procedure as described in 2.80- 2.87, one determines

$$P_-(\alpha) = \frac{\mathrm{i}k(1+f_0)}{N_+(k)N_-(\alpha)} - \frac{\mathrm{i}}{2}\sum_{m=1}^{\infty}\frac{f_m}{(\alpha-\gamma_m)}\frac{\Upsilon_0(\Gamma_m a)}{\Upsilon_0(\Gamma_m d)}\frac{(k+\gamma_m)}{N_+(\gamma_m)}\frac{(k-\alpha)}{N_-(\alpha)} \quad (3.58)$$

with $N_+(\alpha)$ being the usual split function

$$N_+(\alpha) = \sqrt{\frac{2}{\pi d}} \frac{M_+(a,b,\alpha)}{M_+(a,d,\alpha)\, M_+(d,b,\alpha)} \tag{3.59}$$

where the factorization of $M(\rho_1, \rho_2, \alpha)$ is done by following the procedure described in [26]. The unknown coefficients f_m ($m = 0, 1, 2, ...$) can be calculated by taking into account equations 3.48, 3.49 and 3.58 simultaneously, which yields the algebraic system of equations

$$\frac{2k\chi_m}{N_+(k)} f_0 + f_m + \chi_m \sum_{n=1}^{\infty} \frac{f_n}{(\gamma_m + \gamma_n)} \frac{\mathrm{Y}_0(\Gamma_n a)}{\mathrm{Y}_0(\Gamma_n d)} \frac{(k+\gamma_n)(k+\gamma_m)}{N_+(\gamma_n)} = -\frac{2k\chi_m}{N_+(k)} \tag{3.60}$$

for $m = 1, 2, ...$ This explicit statement can be written as,

$$\mathbf{A}\mathbf{f} = \mathbf{B} \tag{3.61}$$

where the elements of $\mathbf{A}$, namely A_{mn} are

$$A_{00} = d \log(d/a) + \frac{1}{[N_+(k)]^2} \tag{3.62}$$

$$A_{m0} = \frac{2k\chi_m}{N_+(k)} \ , \ m = 1, 2, ... \tag{3.63}$$

$$A_{0n} = \frac{1}{N_+(k)\, N_+(\gamma_n)} \frac{\mathrm{Y}_0(\Gamma_n a)}{\mathrm{Y}_0(\Gamma_n d)} \ , \ n = 1, 2, ... \tag{3.64}$$

$$A_{mn} = \begin{cases} 1 + \dfrac{\chi_m}{2\gamma_m} \dfrac{\mathrm{Y}_0(\Gamma_m a)}{\mathrm{Y}_0(\Gamma_m d)} \dfrac{(k+\gamma_m)^2}{N_+(\gamma_m)} & , \quad n = m \\ \dfrac{\chi_m}{(\gamma_m + \gamma_n)} \dfrac{\mathrm{Y}_0(\Gamma_n a)}{\mathrm{Y}_0(\Gamma_n d)} \dfrac{(k+\gamma_n)(k+\gamma_m)}{N_+(\gamma_n)} & , \quad n \neq m \end{cases} \quad , \ m, n = 1, 2, .. \tag{3.65}$$

and the elements of $\mathbf{B}$, namely B_m are

$$B_m = \begin{cases} d\log(d/a) - \dfrac{1}{[N_+(k)]^2} & , \quad m = 0 \\ \\ -\dfrac{2k\chi_m}{N_+(k)} & , \quad m = 1, 2, \ldots \end{cases} \tag{3.66}$$

with

$$\chi_m = \frac{\mathrm{Y}_0(\Gamma_m a)\,\mathrm{Y}_0(\Gamma_m d)}{\gamma_m d N_+(\gamma_m)\left[\mathrm{Y}_0^2(\Gamma_m a) - \mathrm{Y}_0^2(\Gamma_m d)\right]}. \tag{3.67}$$

3.1.3. Analysis of the scattered fields

The scattered field $u_1(\rho, z)$ can be determined by solving the inverse Fourier transform integral

$$u_1(\rho, z) = \frac{1}{2\pi}\int_{\mathcal{L}} F(\rho, \alpha)\,\mathrm{e}^{-\mathrm{i}\alpha z} d\alpha. \tag{3.68}$$

Considering 3.23 and 3.58, the above integral becomes

$$\begin{aligned} u_1(\rho, z) = \frac{\mathrm{i}}{2\pi}\frac{2}{\pi d}\int_{\mathcal{L}} \Bigg\{ & \frac{k(1+f_0)}{N_+(k)} \\ & -\frac{1}{2}\sum_{m=1}^{\infty} \frac{f_m}{(\alpha-\gamma_m)} \frac{\mathrm{Y}_0(\Gamma_m a)}{\mathrm{Y}_0(\Gamma_m d)} \frac{(k+\gamma_m)(k-\alpha)}{N_+(\gamma_m)} \Bigg\} \\ & \times \frac{\pi K L(\rho, b, \alpha)}{2(k^2-\alpha^2) M(d, b, \alpha) N_-(\alpha)} \mathrm{e}^{-\mathrm{i}\alpha z} d\alpha \end{aligned} \tag{3.69}$$

In order to determine the reflected field back to the region $z < 0$, the above integral can be evaluated by virtue of Jordan's lemma and the application of the law of residues, yielding the sum of the residues related to the poles occurring at the simple zeros of $\left(k^2 - \alpha^2\right) M(a, b, \alpha)$ lying in the upper half-plane, namely, at $\alpha = \alpha_n$'s ($n = 0, 1, 2, \ldots$).

Denoting the reflected field as

$$u_1(\rho,z) = R_0\frac{e^{-ikz}}{\rho} + \sum_{n=1}^{\infty} R_n \frac{\pi}{2} K_n \left[\mathrm{J}_1(K_n\rho)\,\mathrm{Y}_0(K_n b) - \mathrm{J}_0(K_n b)\,\mathrm{Y}_1(K_n\rho)\right] e^{-i\alpha_n z} \quad , \quad z<0 \tag{3.70}$$

with

$$K_n = \sqrt{k^2-\alpha_n^2} \tag{3.71}$$

Then, the reflection coefficient R_n is found to be

$$R_n = \left\{ -\frac{k(1+f_0)}{N_+(k)} + \frac{1}{2}\sum_{m=1}^{\infty} \frac{f_m}{(\alpha_n-\gamma_m)} \frac{\mathrm{Y}_0(\Gamma_m a)}{\mathrm{Y}_0(\Gamma_m d)} \frac{(k+\gamma_m)(k-\alpha_n)}{N_+(\gamma_m)} \right\} \times \frac{N_+(\alpha_n)\,M(a,d,\alpha_n)}{K_n^2 M'(a,b,\alpha_n)} \tag{3.72}$$

For the fundamental TEM mode ($n=0$) reflected back to $z<0$, it is found

$$R_0 = \frac{(1+f_0)}{2}\frac{\log(d/a)}{\log(b/a)} \tag{3.73}$$

In a similar fashion, the transmission coefficient can be determined by evaluating the integral in 3.69 for $z>0$ to give

$$u_2(\rho,z) = T_0\frac{e^{-ikz}}{\rho} + \sum_{n=1}^{\infty} T_n \frac{\pi}{2} \xi_n \left[\mathrm{J}_1(\xi_n\rho)\,\mathrm{Y}_0(\xi_n b) - \mathrm{J}_0(\xi_n b)\,\mathrm{Y}_1(\xi_n\rho)\right] e^{i\beta_n z} \quad , \quad z>0 \tag{3.74}$$

with

$$\xi_n = \sqrt{k^2-\beta_n^2} \tag{3.75}$$

and β_n's are the simple zeros of $\left(k^2-\alpha^2\right) M(d,b,\alpha)$, where $\beta_0 = k$. The transmission coefficients T_n's and T_0 are determined as

$$T_n = \left\{ \frac{2k(1+f_0)}{N_+(k)} + \sum_{m=1}^{\infty} \frac{f_m}{(\beta_n+\gamma_m)} \frac{\mathrm{Y}_0(\Gamma_m a)}{\mathrm{Y}_0(\Gamma_m d)} \frac{(k+\gamma_m)(k+\beta_n)}{N_+(\gamma_m)} \right\} \times \frac{1}{\pi d N_+(\beta_n)\xi_n^2 M'(d,b,-\beta_n)} \quad (3.76)$$

and

$$T_0 = \frac{1}{2dN_+(k)\log(b/d)} \left\{ \frac{(1+f_0)}{N_+(k)} + \sum_{m=1}^{\infty} \frac{f_m}{N_+(\gamma_m)} \frac{\mathrm{Y}_0(\Gamma_m a)}{\mathrm{Y}_0(\Gamma_m d)} \right\} \quad (3.77)$$

respectively.

3.2. Mode-Matching Analysis

For the Mode-Matching formulation, the geometry is divided into two regions as depicted in Fig. 3.2, where region A is the part before the step discontinuity defined as $\rho \in (a,b), z < 0$ and region B is the part after the step discontinuitydefined as $\rho \in (d,b), z > 0$.

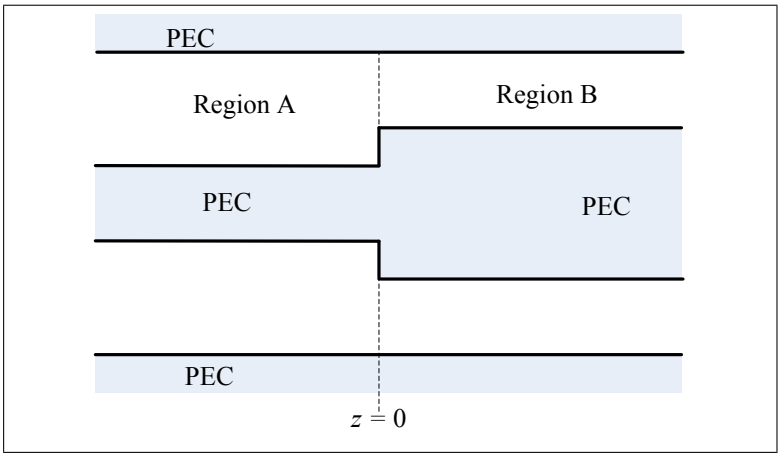

Figure 3.2: Regions for Mode-Matching technique.

The ϕ-component of the total magnetic field at each region is defined as

$$H_{\phi}^{T}=\begin{cases}\dfrac{e^{ikz}}{\rho}+u_{1}\left(\rho,z\right) & ,\quad \rho\in\left(a,b\right),z<0\\ u_{2}\left(\rho,z\right) & ,\quad \rho\in\left(d,b\right),z>0\end{cases} \tag{3.78}$$

where $u_1(\rho,z)$ and $u_2(\rho,z)$ are the scattered fields in region A and region B, respectively. The geometry allows one to expand the field components in terms of their normal modes. Hence, the φ-component of the total magnetic field in region A can be written as

$$H_{\phi}^{A}\left(\rho,z\right)=\frac{\mathrm{e}^{\mathrm{i}kz}}{\rho}+u_{1}\left(\rho,z\right)=\frac{\mathrm{e}^{\mathrm{i}kz}}{\rho}+\sum_{n=0}^{\infty}R_{n}\varphi_{n}\left(\rho\right)e^{-i\alpha_{n}z} \tag{3.79}$$

and, similarly

$$H_{\phi}^{B}\left(\rho,z\right)=u_{2}\left(\rho,z\right)=\sum_{n=0}^{\infty}T_{n}\psi_{n}\left(\rho\right)e^{i\beta_{n}z} \tag{3.80}$$

On the other hand, one can write $\rho-$component of the electric field at related region defined as

$$E_{\rho}^{A}\left(\rho,z\right)=\frac{1}{i\omega\epsilon}\frac{\partial}{\partial z}\left[\frac{\mathrm{e}^{\mathrm{i}kz}}{\rho}+u_{1}\left(\rho,z\right)\right]=\frac{k}{\omega\epsilon}\frac{\mathrm{e}^{\mathrm{i}kz}}{\rho}-\sum_{n=0}^{\infty}\frac{\alpha_{n}}{\omega\varepsilon}R_{n}\varphi_{n}\left(\rho\right)e^{-i\alpha_{n}z} \tag{3.81}$$

and

$$E_{\rho}^{B}\left(\rho,z\right)=\frac{1}{i\omega\epsilon}\frac{\partial}{\partial z}u_{2}\left(\rho,z\right)=\sum_{n=0}^{\infty}\frac{\beta_{n}}{\omega\varepsilon}T_{n}\psi_{n}\left(\rho\right)e^{i\beta_{n}z} \tag{3.82}$$

with

$$\varphi_{n}\left(\rho\right)=\frac{\pi}{2}K_{n}\left[\mathrm{J}_{1}\left(K_{n}\rho\right)\mathrm{Y}_{0}\left(K_{n}b\right)-\mathrm{J}_{0}\left(K_{n}b\right)\mathrm{Y}_{1}\left(K_{n}\rho\right)\right] \tag{3.83}$$

and

$$\psi_n(\rho) = \frac{\pi}{2}\xi_n \left[\mathrm{J}_1(\xi_n \rho)\, \mathrm{Y}_0(\xi_n b) - \mathrm{J}_0(\xi_n b)\, \mathrm{Y}_1(\xi_n \rho) \right] \tag{3.84}$$

The eigenfunctions in the Fourier-Bessel series in 3.79 and 3.80 are determined, such that $u_1(\rho, z)$ and $u_2(\rho, z)$ are the solution of the Helmholtz equation, satisfying the boundary conditions given by:

$$u_1(a, z) + a\frac{\partial}{\partial \rho} u_1(a, z) = 0 \tag{3.85}$$

$$u_1(b, z) + b\frac{\partial}{\partial \rho} u_1(b, z) = 0 \tag{3.86}$$

$$u_2(b, z) + b\frac{\partial}{\partial \rho} u_2(b, z) = 0 \tag{3.87}$$

and

$$u_2(d, z) + d\frac{\partial}{\partial \rho} u_2(d, z) = 0 \tag{3.88}$$

Applying the continuity relations at $z = 0$ yields

$$E_\rho^A(\rho, 0) = \begin{cases} 0 & , \quad a < \rho < d \\ E_\rho^B(\rho, 0) & , \quad d < \rho < b \end{cases} \tag{3.89}$$

and

$$H_\phi^A(\rho, 0) = H_\phi^B(\rho, 0) \quad d < \rho < b. \tag{3.90}$$

Substituting 3.81 and 3.82 into 3.89 yields the following equation.

$$-\frac{k}{\omega\varepsilon}\frac{1}{\rho}+\sum_{n=0}^{\infty}\frac{\alpha_n}{\omega\varepsilon}R_n\varphi_n(\rho)=\sum_{n=0}^{\infty}\frac{\beta_n}{\omega\varepsilon}T_n\psi_n(\rho)\ ,\quad \rho\in(a,b) \tag{3.91}$$

Multiplying 3.91 by $\omega\varepsilon\varphi_m(\rho)$ and integrating along $a<\rho<b$ yields

$$\alpha_m R_m Q_m^{(1)}+\sum_{n=0}^{\infty}\beta_n T_n \Delta_{mn}^{(1)}=kU_m^{(1)}\ ,\ m=0,1,2,...\infty \tag{3.92}$$

with

$$U_m^{(1)}=\int_a^b \varphi_m(\rho)\,d\rho \tag{3.93}$$

$$Q_m^{(1)}=\int_a^b \varphi_n(\rho)\,\varphi_m(\rho)\,\rho d\rho \tag{3.94}$$

$$\Delta_{mn}^{(1)}=\int_d^b \psi_n(\rho)\,\varphi_m(\rho)\,\rho d\rho \tag{3.95}$$

Similarly, after substituting 3.79 and 3.80 into 3.90 and multiplying the related equation by $\omega\varepsilon\psi_m(\rho)$ and integrating along $d<\rho<b$ yields

$$-\sum_{n=0}^{\infty}R_n\Delta_{mn}^{(2)}+T_m Q_m^{(2)}=U_m^{(2)}\ ,\ m=0,1,2,...\infty \tag{3.96}$$

with

$$U_m^{(2)}=\int_d^b \psi_m(\rho)\,d\rho \tag{3.97}$$

$$Q_m^{(2)}=\int_d^b \psi_n(\rho)\,\psi_m(\rho)\,\rho d\rho \tag{3.98}$$

$$\Delta_{mn}^{(2)}=\int_d^b \varphi_n(\rho)\,\psi_m(\rho)\,\rho d\rho \tag{3.99}$$

The sets of equations given by 3.92 and 3.96 must be regarded as a doubly infinite set of equations that must be solved simultaneously. On the other hand, the solution of this doubly infinite set of equations entails truncating the first and the second equations with a truncation number such P and Q, respectively.

$$\alpha_m R_m Q_m^{(1)} + \sum_{n=0}^{N} \beta_n T_n \Delta_{mn}^{(1)} = k U_m^{(1)} \ , \ m = 0, 1, 2, ...P \tag{3.100}$$

$$T_m Q_m^{(2)} - \sum_{n=0}^{N} R_n \Delta_{mn}^{(2)} = U_m^{(2)} \ , \ m = 0, 1, 2, ...Q \tag{3.101}$$

The explicit expressions for $\Delta_{mn}^{(1)}$, $\Delta_{mn}^{(2)}$, $Q_m^{(1)}$, $Q_m^{(2)}$, $U_m^{(1)}$ and $U_m^{(2)}$ are

$$\Delta_{mn}^{(1)} = \begin{cases} \log(b/d) & , \ m = 0, n = 0 \\ 0 & , \ m = 0, n \neq 0 \\ -\dfrac{\pi}{2} \mathrm{V}_m^{(1)} & , \ m \neq 0, n = 0 \\ \dfrac{\pi}{2} \dfrac{K_m^2}{\xi_n^2 - K_m^2} \dfrac{\mathrm{Y}_0(\xi_n b)}{\mathrm{Y}_0(\xi_n d)} \mathrm{V}_m^{(1)} & , \ m \neq 0, n \neq 0 \end{cases} \tag{3.102}$$

$$\mathrm{V}_m^{(1)} = [\mathrm{J}_0(K_m b)\, \mathrm{Y}_0(K_m d) - \mathrm{J}_0(K_m d)\, \mathrm{Y}_0(K_m b)] \tag{3.103}$$

$$\Delta_{mn}^{(2)} = \begin{cases} \log(b/d) & , \ m = 0, n = 0 \\ \dfrac{\pi}{2} \mathrm{V}_n^{(2)} & , \ m = 0, n \neq 0 \\ 0 & , \ m \neq 0, n = 0 \\ \dfrac{\pi}{2} \dfrac{K_n^2}{K_n^2 - \xi_m^2} \dfrac{\mathrm{Y}_0(\xi_m b)}{\mathrm{Y}_0(\xi_m d)} \mathrm{V}_n^{(2)} & , \ m \neq 0, n \neq 0 \end{cases} \tag{3.104}$$

$$\mathrm{V}_n^{(2)} = [\mathrm{J}_0(K_n d)\, \mathrm{Y}_0(K_n b) - \mathrm{J}_0(K_n b)\, \mathrm{Y}_0(K_n d)] \tag{3.105}$$

$$Q_m^{(1)} = \begin{cases} \log(b/a) & , \quad m = 0 \\ \dfrac{\left[\mathrm{Y}_0^2(K_m a) - \mathrm{Y}_0^2(K_m b)\right]}{2\mathrm{Y}_0^2(K_m a)} & , \quad m \neq 0 \end{cases} \tag{3.106}$$

$$Q_m^{(2)} = \begin{cases} \log(b/d) & , \quad m = 0 \\ \dfrac{\left[\mathrm{Y}_0^2(\xi_m d) - \mathrm{Y}_0^2(\xi_m b)\right]}{2\mathrm{Y}_0^2(\xi_m d)} & , \quad m \neq 0 \end{cases} \tag{3.107}$$

$$U_m^{(1)} = \begin{cases} \log(b/a) & , \quad m = 0 \\ 0 & , \quad m \neq 0 \end{cases} \tag{3.108}$$

$$U_m^{(2)} = \begin{cases} \log(b/d) & , \quad m = 0 \\ 0 & , \quad m \neq 0 \end{cases} \tag{3.109}$$

4. NUMERICAL RESULTS

In this chapter, the results obtained via both Wiener–Hopf and Mode-Matching techniques are evaluated numerically and compared to each other. Constructing the systems of linear algebric equations obtained in Chapter 2 and Chapter 3 via two methods properly allow one to determine the coefficients R_n and T_n numerically. On the other hand, when there is an only the fundamental TEM mode propagating, the transmission coefficients calculated via Wiener–Hopf and Mode-Matching techniques have the relation

$$T_{0,WienerHopf} = T_{0,Mode-Matching} - 1 \tag{4.1}$$

due to the difference in defining the total field in the two formulations. Considering the Mode-Matching formulation for the outer wall problem at the frequencies where only the fundamental TEM mode is propagating, one can write the field terms H_ϕ and E_ρ in region A ($z < 0$)

$$H_\phi^A = \frac{e^{ikz}}{\rho} + R_0 \frac{e^{-ikz}}{\rho} \ , \ E_\rho^A = \frac{k}{\omega\epsilon}\frac{e^{ikz}}{\rho} - \frac{k}{\omega\epsilon} R_0 \frac{e^{-ikz}}{\rho} \tag{4.2}$$

and in region B ($z > 0$)

$$H_\phi^B = T_0 \frac{e^{ikz}}{\rho} \ , \ E_\rho^B = \frac{k}{\omega\epsilon} T_0 \frac{e^{ikz}}{\rho} \tag{4.3}$$

Considering the general formula for calculating the power

$$P = \frac{1}{2}\mathrm{Re}\left\{ \int\int_S \left(E_\rho^A \hat{a}_\rho \times H_\phi^{A*} \hat{a}_\phi \right) \right\} \cdot \hat{a}_z dS \tag{4.4}$$

where H_ϕ^{A*} is the conjugate of the related term.

The power in regions A and B become

$$P^A = \frac{\pi k}{\omega \epsilon} \left(1 - |R_0|^2\right) \log\left(b/a\right) \tag{4.5}$$

and

$$P^B = \frac{\pi k}{\omega \epsilon} |T_0|^2 \log\left(d/a\right) \tag{4.6}$$

respectively. The conservation of energy yields

$$\left(1 - |R_0|^2\right) \log\left(b/a\right) = \left(|T_0|^2\right) \log\left(d/a\right) \tag{4.7}$$

Following the similar procedure, an analogue equation can be obtained for the inner wall problem.

$$\left(1 - |R_0|^2\right) \log\left(b/a\right) = \left(|T_0|^2\right) \log\left(b/d\right) \tag{4.8}$$

4.1. The Convergence Comparison of the Techniques

Since both Wiener–Hopf and Mode-Matching analysis involve infinite sets of linear algebraic equations, convergence of the solution regarding the truncation number must be illustrated for each technique. The Figures 4.1- 4.4 show the dependence of the magnitudes of the reflection and transmission coefficients R_0 and T_0 to the truncation number N at frequencies $f = 100$ MHz and $f = 4$ GHz for $a = 1$ cm, $b = 3$ cm and $d = 10$ cm. These figures show that the Wiener–Hopf technique provides a better convergence than the Mode-Matching technique.

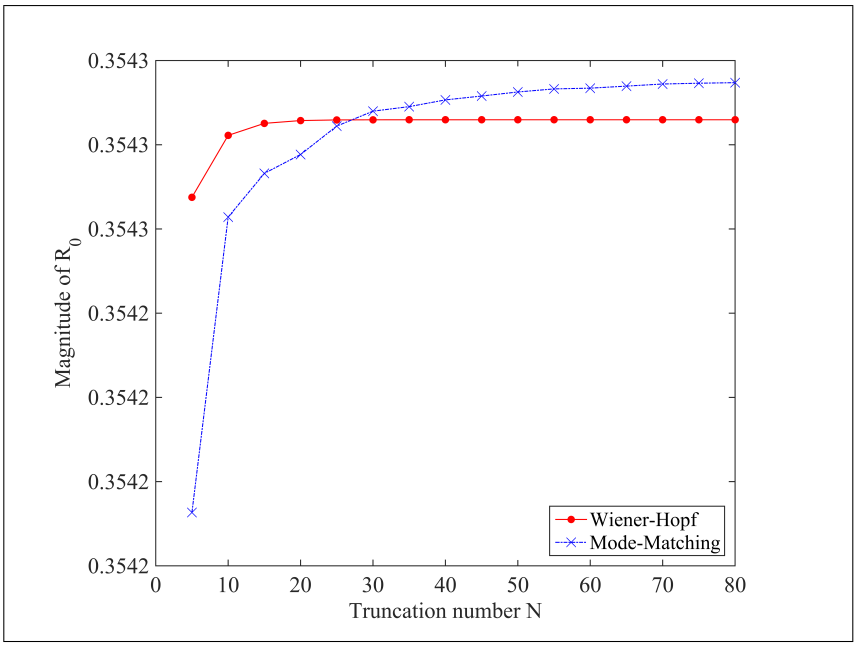

Figure 4.1: Convergence of $|R_0|$ at $f = 100$ MHz

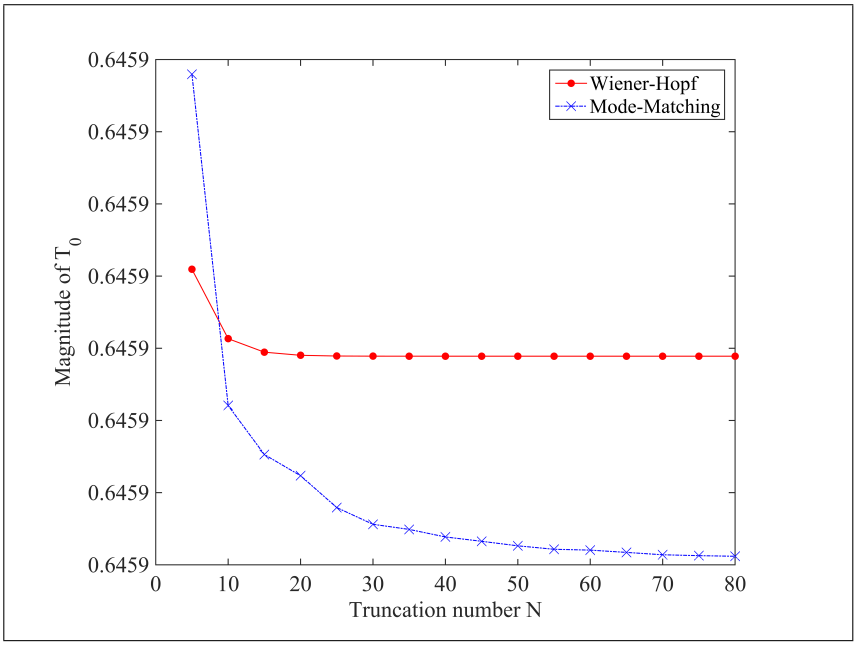

Figure 4.2: Convergence of $|T_0|$ at $f = 100$ MHz

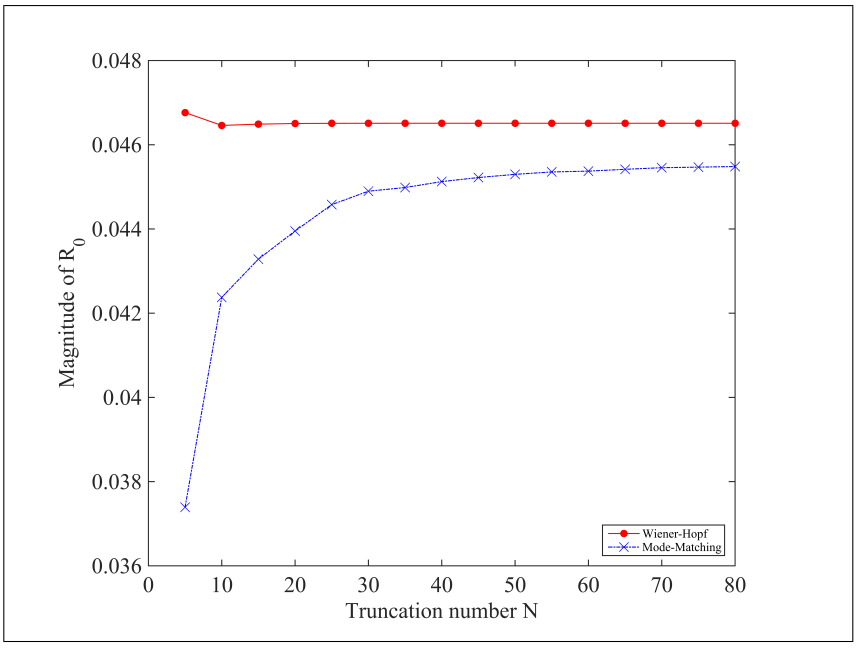

Figure 4.3: Convergence of $|R_0|$ at $f = 4$ GHz

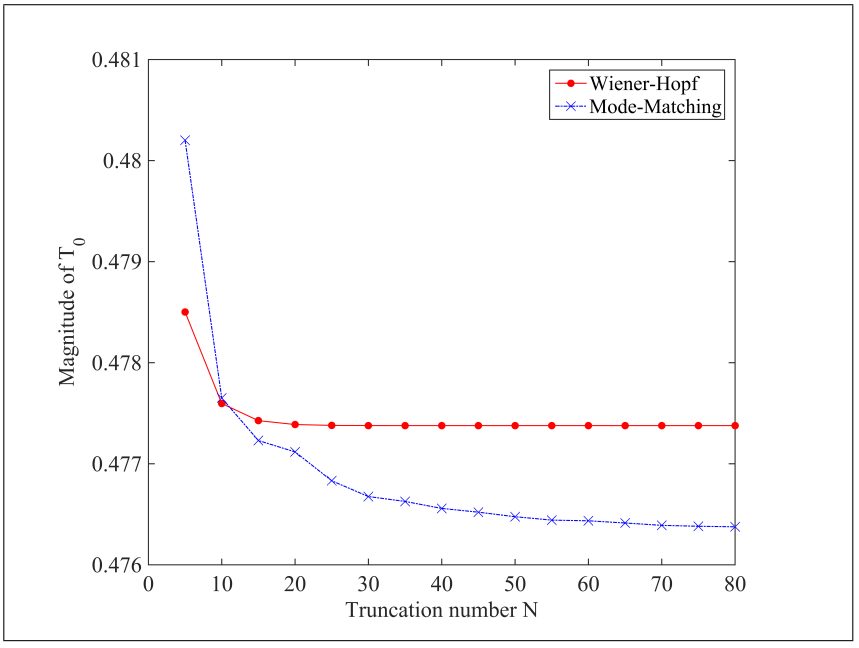

Figure 4.4: Convergence of $|T_0|$ at $f = 4$ GHz

This issue is well known in the literature as the lack of edge conditions in 2.12 and therefore the Mode-Matching technique causes slower convergence. Since the Wiener–Hopf technique is converging faster, the computation time for this technique is less compared to the Mode-Matching technique.

4.2. Scattering Coefficients of the Outer Wall Problem

In this section the results obtained via both Wiener-Hopf and Mode-Matching techniques are evaluated numerically for the problem of step discontinuity on the outer wall.

During the numerical analysis, one needs to calculate the zeros of the functions $M(a,b,\alpha), M(a,d,\alpha)$ and $M(b,d,\alpha)$. Note that these functions are related to the kernel function $N(\alpha)$ of the Wiener-Hopf equation given in 2.76 which characterizes the nature of the step discontinuity on the outer wall of a coaxial waveguide. If $M(a,b,\alpha)$ is analyzed asymptotically for large $|a|$ by taking into account

$$\mathrm{J}_0(z) \simeq \sqrt{\frac{2}{\pi z}} \cos\left(z - \frac{\pi}{4}\right) \quad , \text{ for large } |z| \tag{4.9}$$

and

$$\mathrm{Y}_0(z) \simeq \sqrt{\frac{2}{\pi z}} \sin\left(z - \frac{\pi}{4}\right) \quad , \text{ for large } |z| \tag{4.10}$$

In this respect, one gets the eigenvalue equation

$$\sin\left[K_m(b-a)\right] = 0 \ , \ m = 1,2,... \tag{4.11}$$

where

$$K_m \simeq \frac{m\pi}{(b-a)} \ , \ m = 1,2,... \tag{4.12}$$

Thus, for the zeros of $M(a,d,\alpha)$ one finds,

$$\xi_m \simeq \frac{m\pi}{(d-a)} \ , \ m = 1,2,... \tag{4.13}$$

and

$$\beta_m = \sqrt{k^2 - \xi_m^2} \ , \ m = 1, 2, ... \tag{4.14}$$

Here α_m's and β_m's correspond to the wavenumbers of higher-order modes associated with their indices in the regions A and B, respectively. Hence, the corresponding modes are propagating only when these wavenumbers become purely real. Note that, the righthand sides of the equations 4.13 and 4.14 are only the asymptotic expressions for K_m and ξ_m. The details in variations of $M(a, b, \alpha)$ and $M(a, d, \alpha)$ with respect to $K(\alpha)$ are illustrated in [28].

On the other hand, the asymptotic expression for the zeros of $M(b, d, \alpha)$ can be found in a similar fashion to give,

$$\Gamma_m \simeq \frac{m\pi}{(d-b)} \ , \ m = 1, 2, ... \tag{4.15}$$

and

$$\gamma_m = \sqrt{k^2 - \Gamma_m^2} \ , \ m = 1, 2, ... \tag{4.16}$$

Reader in this section finds the computational results of the scattering coefficients showing the effect of the ratio of cross-sectional areas for frequencies up to 10 MHz, 1.5 GHz and 4 GHz respectively, where the excitation is the incident TEM wave given by 2.1. In all the figures, the area ratio defined by

$$\text{Area ratio} = \frac{S_2}{S_1} = \frac{d^2 - a^2}{b^2 - a^2} \tag{4.17}$$

is 12.375 for the blue line, 6.6 for the green line, and 4.125 for the red line.

The truncation number N is chosen as 40 and 80 for Wiener–Hopf and Mode-Matching analysis, respectively. In addition, the straight lines in the graphs indicate the Wiener–Hopf technique, while the dashed lines with a marker demonstrate the Mode-Matching technique.

It can be observed in Figures 4.5- 4.14 that the two methods, i.e., the Wiener–Hopf and Mode-Matching techniques, have very good agreement. Besides, one can conclude that when the area ratio increases, the magnitude of the reflection coefficient also increases while the magnitude of the transmission coefficient decreases. This means that when the area ratio is increased, more energy is reflected back and less is transmitted to region B.

In addition, the same trend is observed in Figures 4.9-4.12 regarding the return and insertion losses for the same area ratios, which are calculated directly by

$$RL = -20 \log |R_0| \tag{4.18}$$

and

$$IL = -20 \log |T_0| \tag{4.19}$$

respectively, with the unit dB.

The graphs related to the RL and IL demonstrate that when the area ratio is increased, more energy is reflected back and less is transmitted to region B. The Figures 4.5, 4.7, 4.9 and 4.11 are of special interest due to the need of low frequency electromagnetic modelling of the measurement setup described in [2].

Additionally, the magnitude of the reflection and transmission coefficients are presented in Figs.4.13 and 4.14 upto 4GHz, where two additional TM modes are observed to start propagating in region B after their relevant cut-off frequencies 1.62 GHz and 3.31 GHz are exceed. When new modes start to propagate, the energy carried by the fundamental TEM mode is obviously decreased dramatically.

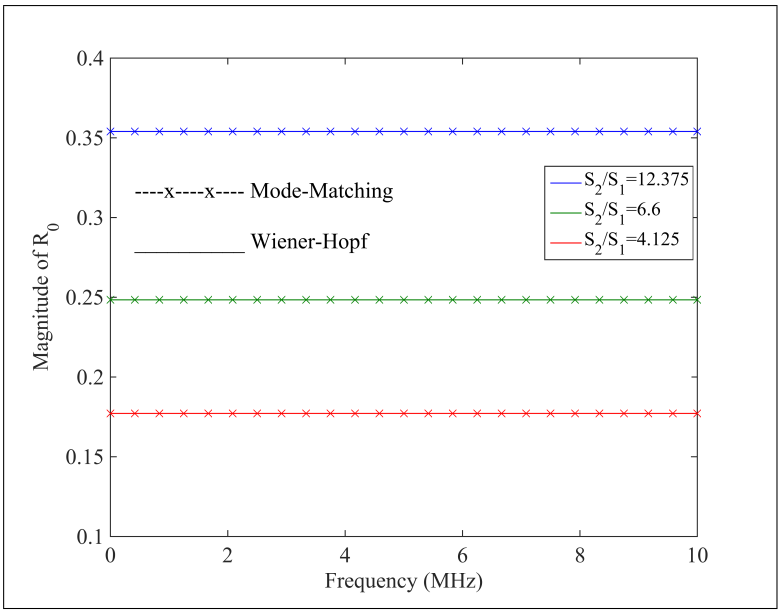

Figure 4.5: Magnitude of R_0 upto $f = 10$ MHz.

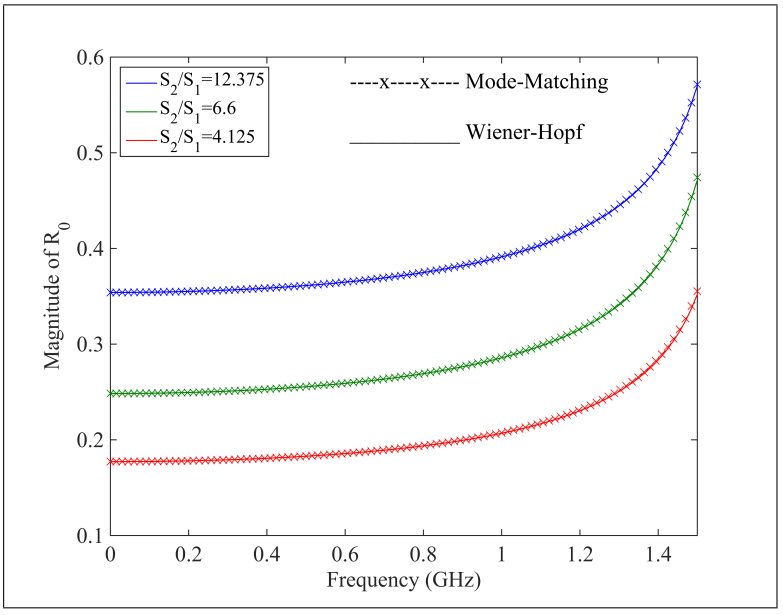

Figure 4.6: Magnitude of R_0 upto $f = 1.5$ GHz.

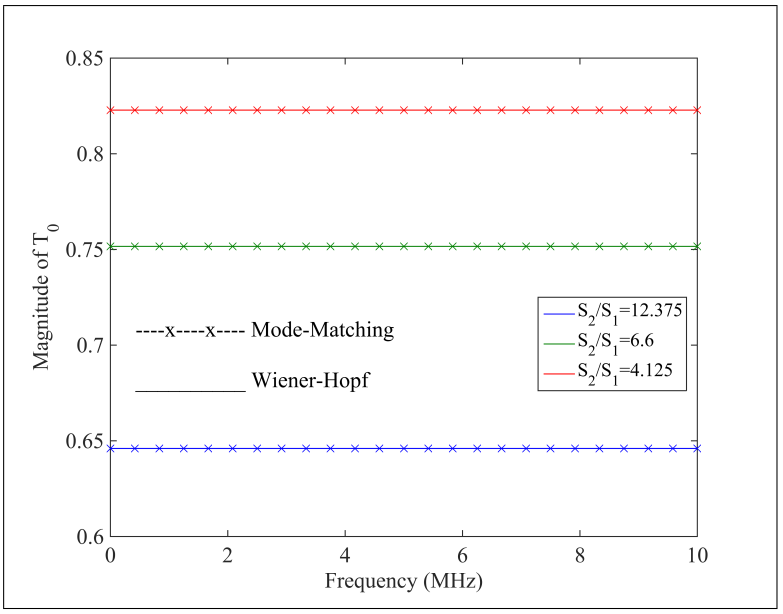

Figure 4.7: Magnitude of T_0 upto $f = 10$ MHz.

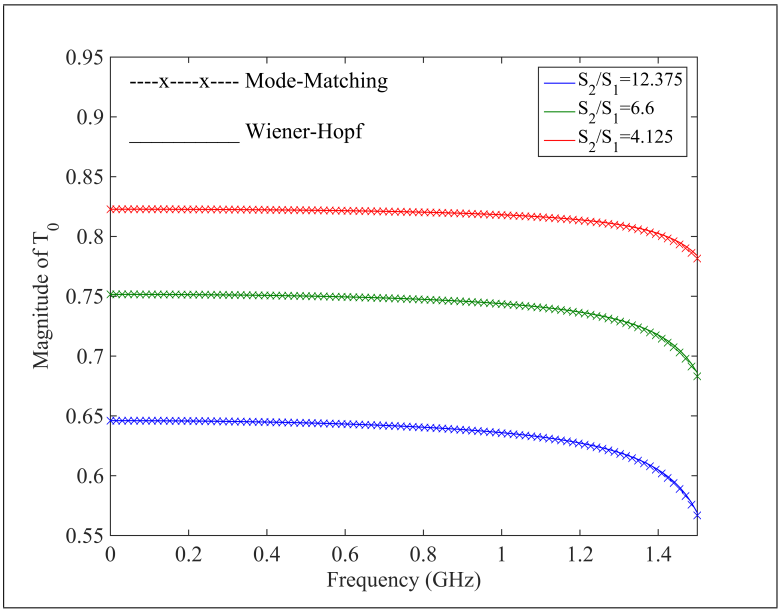

Figure 4.8: Magnitude of T_0 upto $f = 1.5$ GHz.

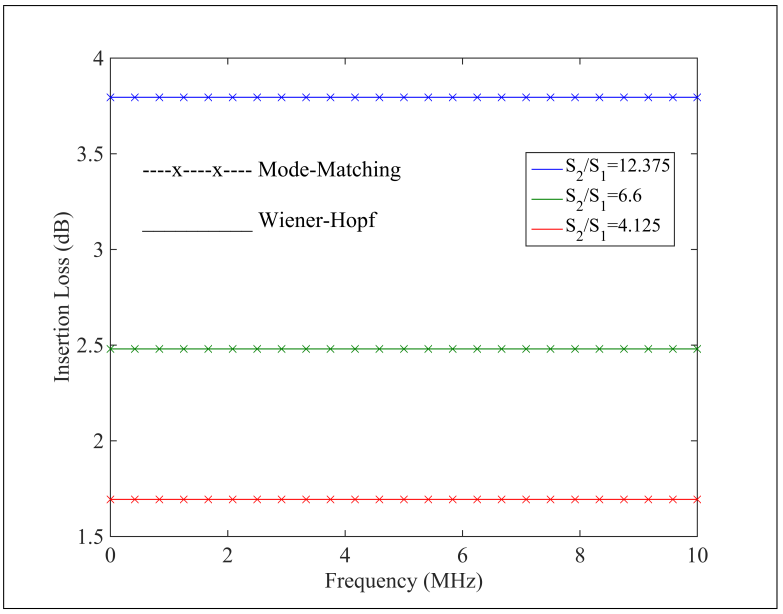

Figure 4.9: Insertion loss upto $f = 10$ MHz.

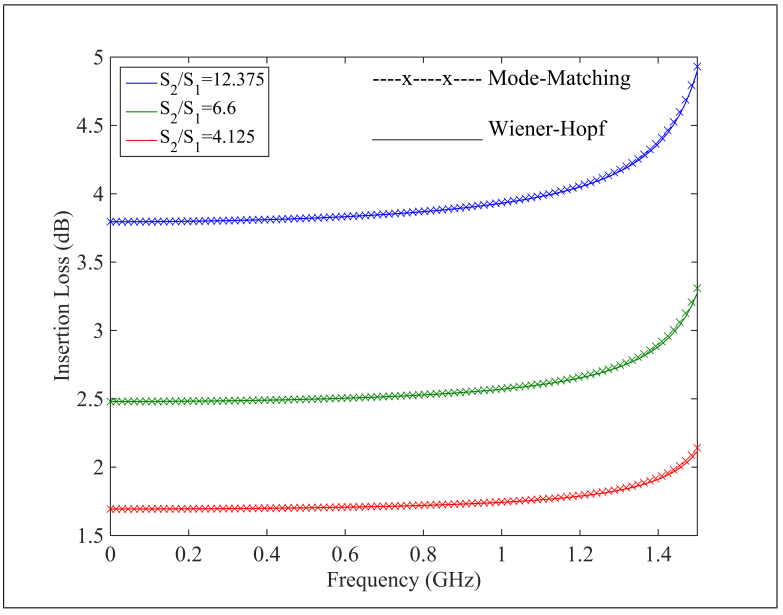

Figure 4.10: Insertion loss upto $f = 1.5$ GHz.

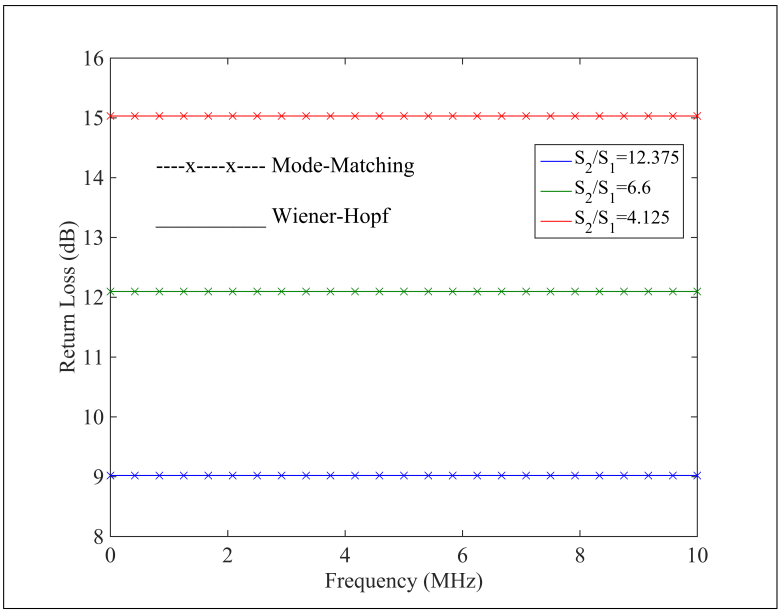

Figure 4.11: Return loss upto $f = 10$ MHz.

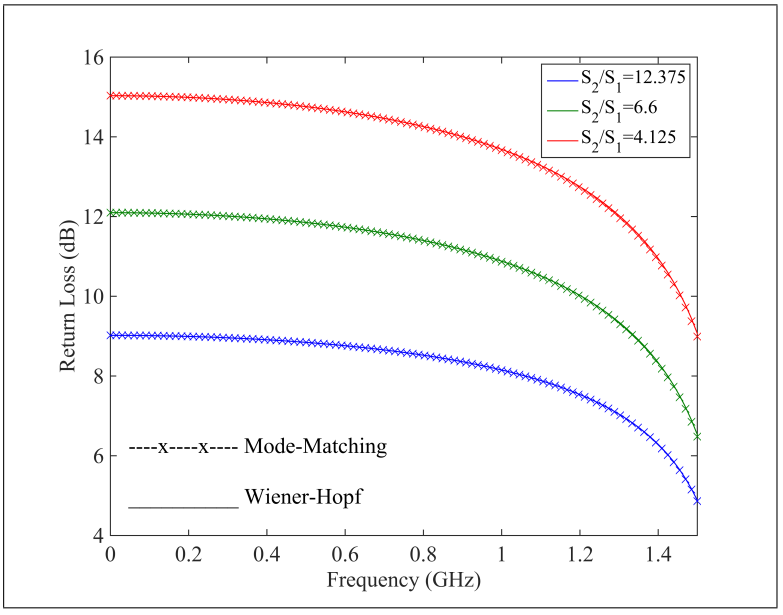

Figure 4.12: Return loss upto $f = 1.5$ GHz.

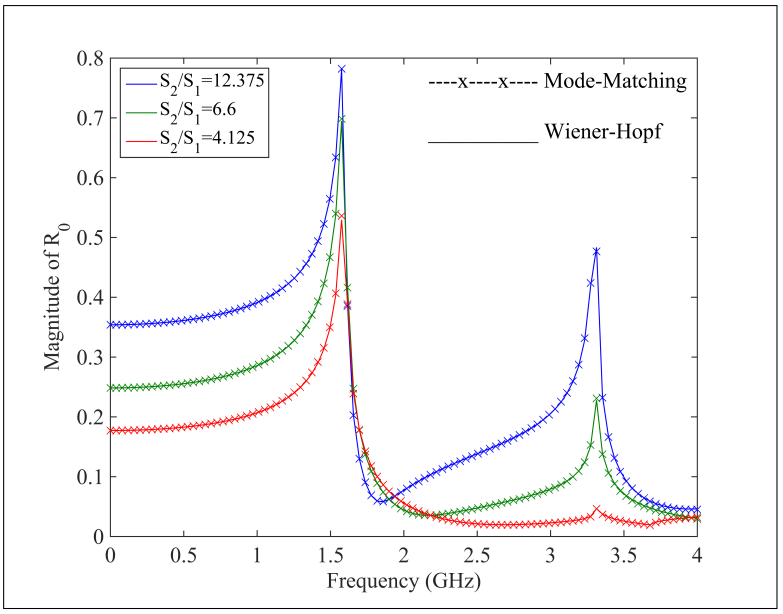

Figure 4.13: Magnitude of R_0 upto $f = 4$ GHz.

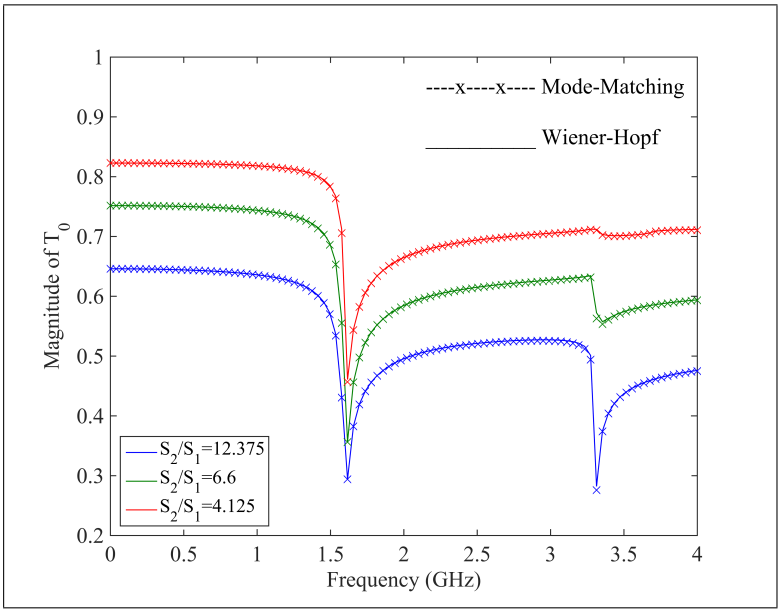

Figure 4.14: Magnitude of T_0 upto $f = 4$ GHz.

4.3. Scattering Coefficients of the Inner Wall Problem

Reader in this section finds the computational results of the scattering coefficients showing the effect of the ratio of cross-sectional areas of the inner wall problem for frequencies up to 10MHz, 1.5 GHz and 4 GHz respectively, where the excitation is the incident TEM wave given by (2.1). In all the figures, the area ratio defined by

$$\text{Area ratio} = \frac{S_2}{S_1} = \frac{b^2 - d^2}{b^2 - a^2} \tag{4.20}$$

is 0.9192 for the blue line, 0.8485 for the green line, and 0.7575 for the red line. Similar to previous problem, the truncation number N is chosen as 40 and 80 for Wiener–Hopf and Mode-Matching analysis, respectively.

It can be observed in Figures 4.15- 4.24 that the two methods, i.e., the Wiener–Hopf and Mode-Matching techniques, have very good agreement, especially at low frequencies. On the other hand, contrary to the results of the outer wall problem, one can conclude that when the area ratio increases, the magnitude of the reflection coefficient also decreases while the magnitude of the transmission coefficient increases. This means that when the area ratio is increased, less energy is reflected back and more is transmitted to region B. Same trend is also observed in Figures 4.19-4.22 regarding RL and IL terms.

Additioanlly, the magnitude of the reflection and transmission coefficients are presented in Figs.4.23 and 4.24 upto 4GHz, where two additional TM modes are observed to start propagating in region A after their relevant cut-off frequencies 1.62 GHz and 3.31 GHz are exceed. When new modes start to propagate, the energy carried by the fundamental TEM mode is obviously decreased dramatically.

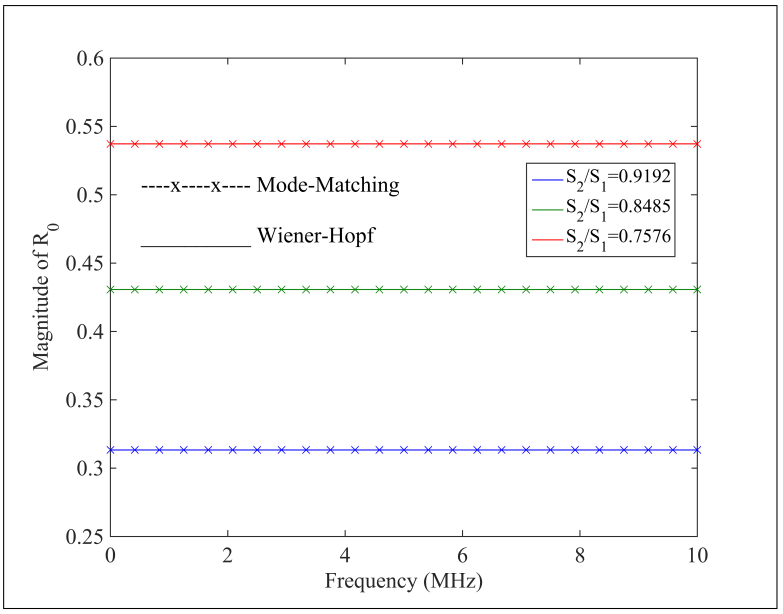

Figure 4.15: Magnitude of R_0 upto $f = 10$ MHz.

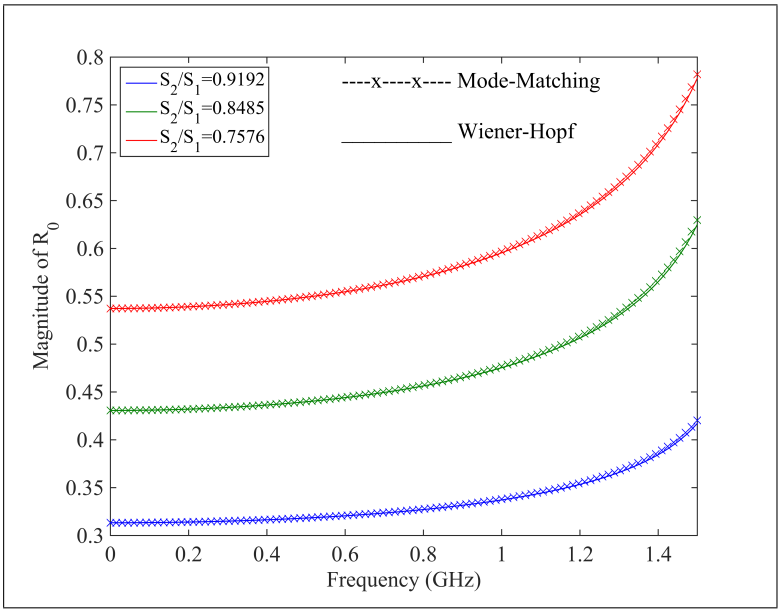

Figure 4.16: Magnitude of R_0 upto $f = 1.5$ GHz.

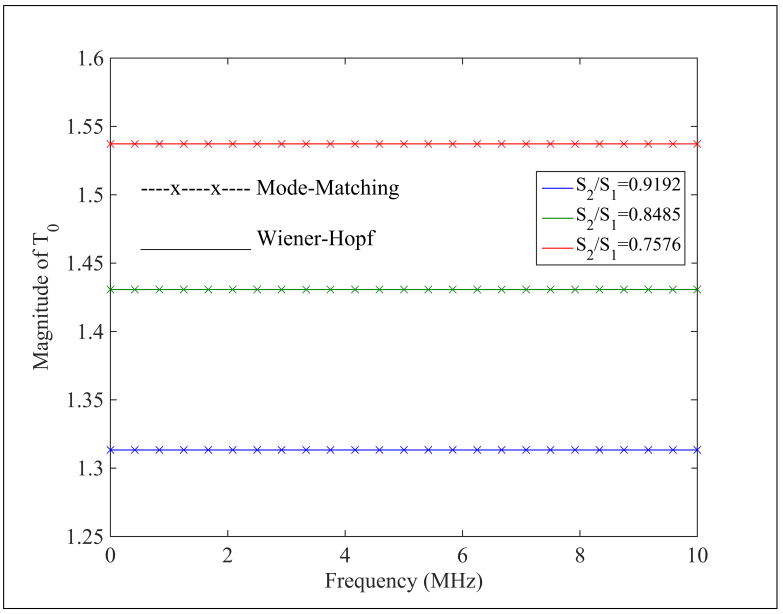

Figure 4.17: Magnitude of T_0 upto $f = 10$ MHz.

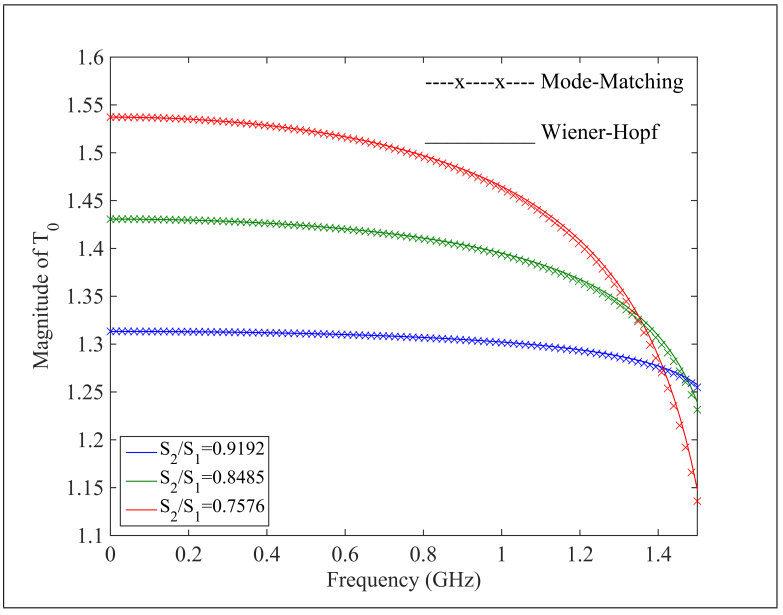

Figure 4.18: Magnitude of T_0 upto $f = 1.5$ GHz.

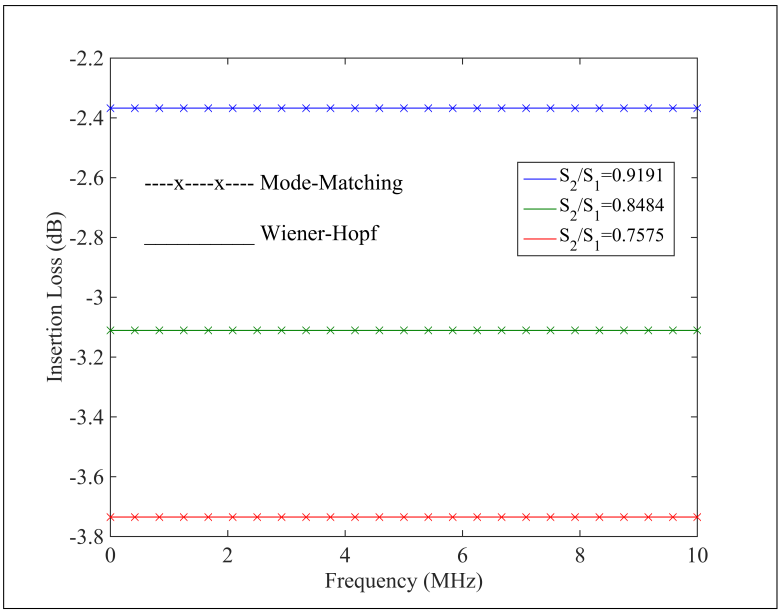

Figure 4.19: Insertion loss upto $f = 10$ MHz.

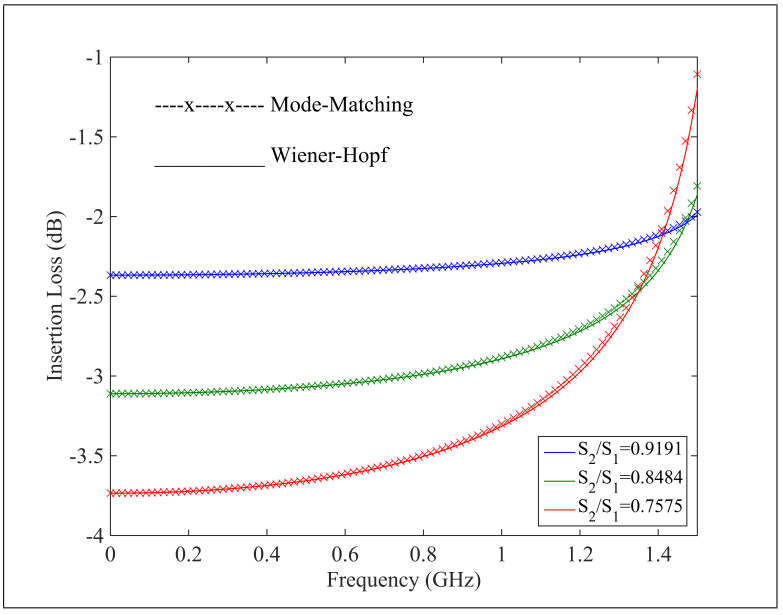

Figure 4.20: Insertion loss upto $f = 1.5$ GHz.

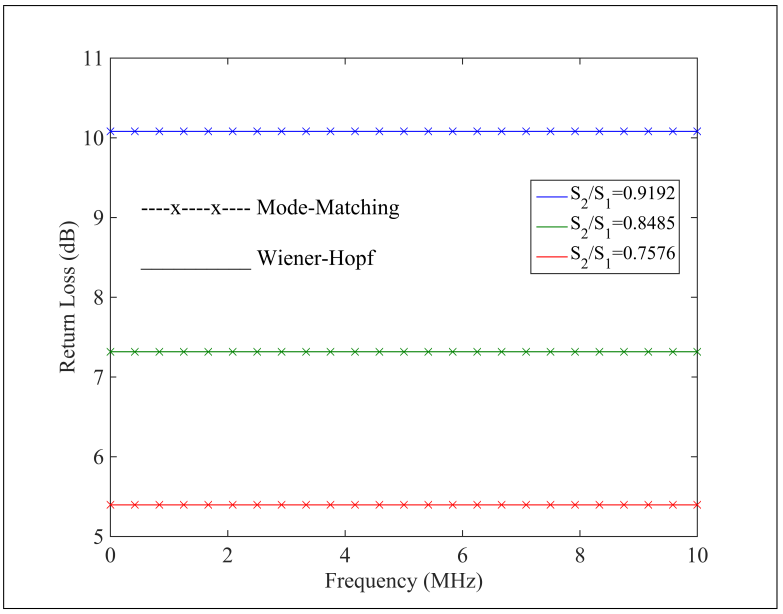

Figure 4.21: Return loss upto $f = 10$ MHz.

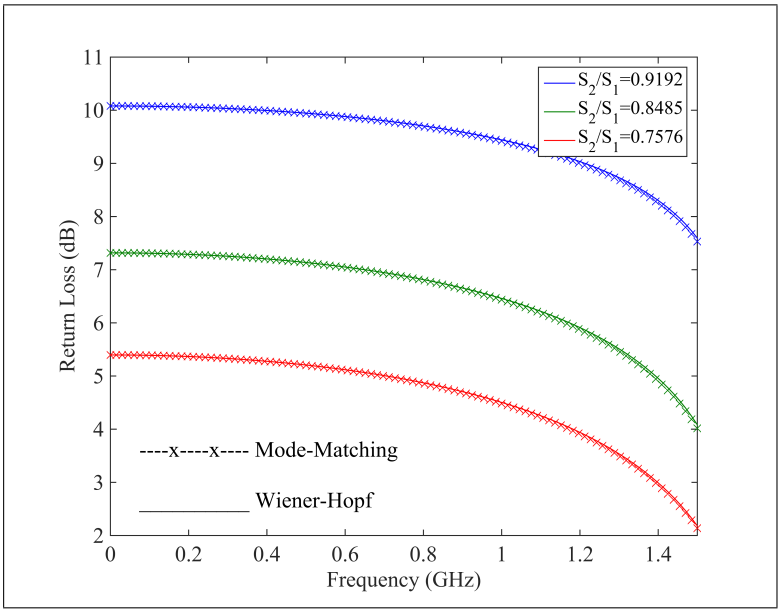

Figure 4.22: Return loss upto $f = 1.5$ GHz.

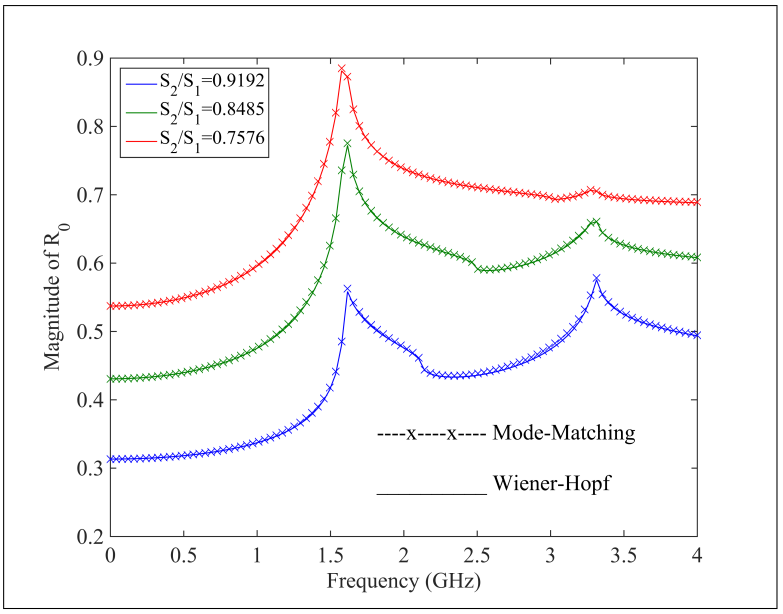

Figure 4.23: Magnitude of R_0 upto $f = 4$ GHz.

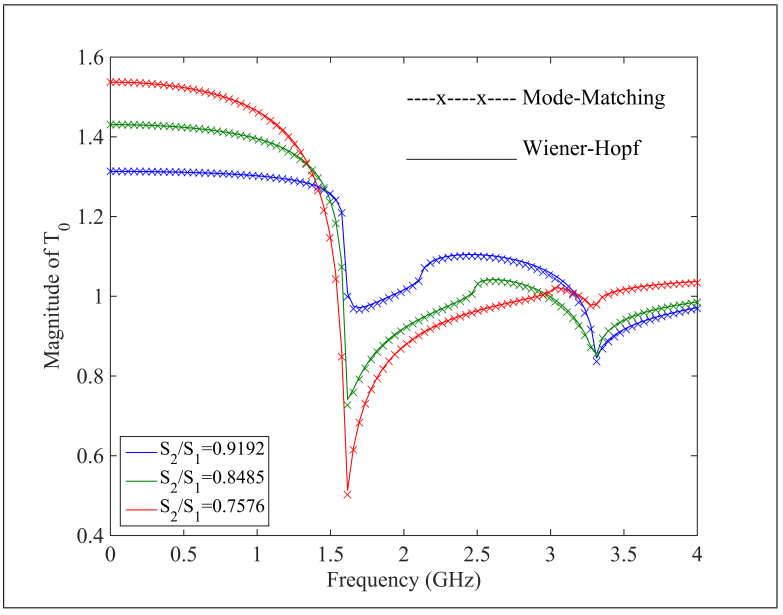

Figure 4.24: Magnitude of T_0 upto $f = 4$ GHz.

5. CONCLUSION

Engineering applications of coaxial waveguides involving discontinuities -such as a abrupt step on the outer or inner conductor wall- have received considerable attention since many decades, and an accurate evaluation of the behaviours of electromagnetic waves along these cables is essential for practical purposes.

In this thesis, the propagation of TEM waves along a coaxial waveguide with a step discontinuity on its outer and inner walls has been analyzed by applying the Wiener-Hopf and Mode-Matching techniques, both of which are considered to be rigorous analyses in frequency domain.

First, at the beginning of the analysis, the geometry of step discontinuity on the outer wall problem is reduced into an equivalent two dimensional one in the virtue of axial symmetry. Then, the Wiener-Hopf technique is applied to this problem by considering the Helmholtz equation, boundary conditions, and continuity relations in the Fourier transform domain, and a modified Wiener-Hopf equation of the second type is derived. This MWHE also contains a unique kernel function representing the area expansion, i.e, the step discontinuity on the outer wall. It is solved according to the related method and the obtained solution is form of an algebraic system of equations. At final stage, this algebraic system is evaluated approximately by following the numerical procedure and the scattering coefficients are derived.

Second, the Mode-Matcing technique is employed to analyze the same geometry, and a doubly infinite set of equations is found at the end of the method, which must be solved simultaneously. This system is solved by truncating both equations with a truncation number such P and Q. At the and of the analysis, the explicit statements are obtained for each equation.

Third, following a similar procedure, the problem of step discontinuity on the inner wall is formulated and solved by the Wiener-Hopf and Mode-Matching techniques, and the scattering coefficients are determined.

Fourth, i.e, the computational part of this study, a computer code is developed in MATLAB by using the approximate statements and the related equations for each problem and for each method, and then the graphs are produced to visualize the numerical results. The Figures 4.1-4.4 show that the Wiener-Hopf technique provides

a better convergence than the Mode-Matching technique. In other words, the Mode-Matching technique causes slower convergence due to the well known issue in the literature as the lack of edge conditions in 2.12. In this respect, the Wiener-Hopf technique is converging faster and the computation time for this method is less compared to the Mode-Matching technique.

In the Figures 4.6-4.15, the reflection and transmission coefficients demonstrating the effect of the area expansion are illustrated for frequencies up to 10 MHz, 1.5 GHz and 4 GHz respectively, where the excitation is the incident TEM wave. Note that the truncation number N is chosen as 40 and 80 for Wiener-Hopf and Mode-Matching calculation, respectively. It is clearly seen in these figures that the two methods, i.e., the Wiener-Hopf and Mode-Matching techniques, have very good agreement. It is interesting to note that although the lack of edge conditions, the accuracy of the Mode-Matching technique is great, especially for low frequencies. This information is very useful for the application of the Mode-Matching technique in more complex problems, where the Wiener-Hopf technique cannot be applicable.

In addition, by evaluating these figures one can conclude that when the area ratio increases, the magnitude of the reflection coefficient also increases while the magnitude of the transmission coefficient decreases. This means that when the area ratio is increased, more energy is reflected back and less is transmitted to region B. This phenomena can also observed from the figures related to the return and insertion losses for the same area ratios. Besides, Figures 4.14 and 4.15 indicate that two additional TM modes start propagating in region B after their relevant cut-off frequencies are exceed, and therefore the energy carried by the fundamental TEM mode is obviously decreased dramatically. Same phenomena and the law of conversation of energy as well can be observed in the Figure 4.5.

The effects of the area expansion are illustrated in Figures 4.16-4.25 for the inner wall problem as well. In contrast to the results of the first problem, the area ratio increases, the magnitude of the reflection coefficient decreases while the magnitude of the transmission coefficient increases. In other words, the area expansion of the region B is increased, less energy is reflected back and more is transmitted to region B, et vice versa.

These results constructs a solid knowledge of the effect of a step discontinuity on

the outer and inner walls of a coaxial waveguide on the propagation of TEM waves. These types of scattering mechanisms are among the many occurring in the measurement setup described in [2]. In particular, these results illustrate the great importance of an area change in the modelling of connector mismatch at low frequencies. Additionally, the comparison of these two techniques provides an understanding on the use of the Wiener-Hopf and Mode-Matching techniques for future studies which involving more complex geometries, and these different scattering mechanisms will be subject of forthcoming studies by the author.

REFERENCES

[1] Markuvitz N., (1965), "Waveguide Theory", 1th Edition, Dower Publication.

[2] Nordebo S., Nilsson B., Biro T., Çınar G., Gustafsson M., Gustafsson S., Karlsson A., Sjöberg M., (2011), "Wave modeling and fault localization for underwater power cables", 13th International Conference on Electromagnetics in Advanced Applications, 698-701, Torino, Italy, 12-16 September

[3] Whinnery J. R., Jamieson H. W., Robbins T. E., (1944), "Coaxial-line discontinuities", Proceedings of the Institute of Radio Engineers, 32 (11), 695-709.

[4] Green H. E., (1965), "The Numerical solution of some important transmission-line problems", IEEE Transactions on Microwave Theory and Techniques, 13 (5), 676-692.

[5] Eom H. J., Noh Y. C., Park J. K., (1998), "Scattering analysis of a coaxial line terminated by a gap", IEEE Microwave and Guided Wave Letters, 8 (6), 218-219.

[6] Mongiardo M., Russer P., Dionigi M., Felsen L. B., (1998), "Waveguide step discontinuities revisited by the generalized network formulation", IEEE MTT-S International Microwave Symposium Digest, 917-920, Baltimore, Maryland, USA, 7-12 June

[7] Yu W., Mittra R., Dey S., (2001), "Application of the nonuniform FDTD technique to analysis of coaxial discontinuity structures", IEEE Transactions on Microwave Theory and Techniques, 49 (1), 207-209.

[8] Obrzut J., Anopchenko A., (2004), "Input impedance of a coaxial line terminated with a complex gap capacitance - numerical and experimental analysis", IEEE Transactions on Instrumentation and Measurement, 53 (4), 1197-1201.

[9] Fallahi A., Rashed-Mohassel J., (2006), "Dyadic Green function for a step discontinuity in a coaxial cable", 11th Int. Conference on Mathematical Methods in Electromagnetic Theory, 402-404, Kharkiv, Ukraine, 26-29 June.

[10] Aksoy S., Tretyakov O. A., (2003), "Evolution equations for analytical study of digital signals in waveguides", Journal of Electromagnetic Waves and Applications, 17 (12), 665–1682.

[11] Butrym A. Y., Zheng Y., Tretyakov O. A., (2004), "Transient diffraction on a permittivity step in a waveguide: Closed-form solution in time domain Journal of Electromagnetic Waves and Applications, 18 (7), 861–876.

[12] Pazynin V. L., Sirenko K. Y., (2006), "The strong approach to analysis of transients in the axially symmetrical waveguide units," Telecommunications and Radio Engineering., 65 (1), 1–18.

[13] Çinar G., Büyükaksoy A., (2006), "A hybrid method for the solution of plane wave diffraction by an impedance loaded parallel plate waveguide", Progress in Electromagnetic Research, 293–310, Tokyo, Japan, 2-5 August.

[14] Daniele V. G., Montrosset I., Zich R. S., (1979), "Wiener–Hopf solution for the junction between a smooth and a corrugated cylindrical waveguide", Radio Science, 14 (6), 943–955.

[15] Kuryliak D. B., Koshikawa S., Kobayashi K., Nazarchuk Z. T., (2000), "Wiener–Hopf analysis of the vector diffraction problem for a cylindrical waveguide cavity", International Conference on Mathematical Methods in Electromagnetic Theory, 694–696, Kharkov, Ukraine, 12-15 September.

[16] Alkumru A., Büyükaksoy A, Günes F., (2002), "Wiener–Hopf analysis of the dominant mode propagation in a dual-ridged parallel plate waveguide with impedance loading", Electromagnetics, 22 (1), 37–58.

[17] Tayyar I. H., Büyükaksoy A., Isikyer A, (2008), "Wiener–Hopf analysis of the parallel plate waveguide with opposing rectangular dielectric-filled grooves", Canadian Journal of Physics, 86 (5), 733–745.

[18] Mittra R., Lee S. W., (1971), "Analytical Techniques in the Theory of Guided Waves", 2nd Edition, McMillan

[19] Wexler A., (1967), "Solution of waveguide discontinuities by modal analysis" IEEE Transactions on Microwave Theory and Techniques, 15 (9), 508–517.

[20] Alessandri F., Bartolucci G., Sorrentino R., (1988), "Admittance matrix formulation of waveguide discontinuity problems: Computer-aided design of branch guide directional couplers", IEEE Transactions on Microwave Theory and Techniques, 36 (2), 394–403.

[21] Eleftheriades G. V., Omar A. S., Rebeiz L. P. B. K. M., (1994), "Some important properties of waveguide junction generalized scattering matrices in the context of the mode matching technique", IEEE Transactions on Microwave Theory and Techniques, 42 (10), 1896–1903.

[22] Orfanidis A. P., Kyriacou G. A., Sahalos J. N., (2000), "A mode-matching technique for the study of circular and coaxial waveguide discontinuities based on closed-form coupling integrals", IEEE Transactions on Microwave Theory and Techniques, 48 (5), 880–883.

[23] Huang R. F., Zhang D. M., (2007), "Application of mode matching method to analysis of axisymmetric coaxial discontinuity structures used in permeability and/or permittivity measurement", Progress in Electromagnetic Research, 67, 205–230.

[24] Ross S. L., (1984), “Differential Equations”, 3rd Edition, Wiley.

[25] Bender C. M., Orszag S. A., (1999), “Advanced mathematical methods for scientists and engineers: Asymptotic Methods and Perturbation Theory”, 1st Edition, Springer-Verlag.

[26] Rawlins A. D., (1995), “A bifurcated circular waveguide problem”, IMA Journal of Applied Mathematics, 54 (1), 59–81.

[27] İdemen M., (2008), “Kompleks Değişkenli Fonksiyonlar Teorisi”, 1. Baskı, İstanbul Teknik Ünivesitesi Vakfı Yayınları.

[28] Aksimsek S., Çinar G., Nilsson B., Nordebo S., (2012), “TEM wave propagation in a coaxial cable with a step discontinuity on the outer wall”, Technical Report No: urn:nbn:se:lnu:diva-22677, School of Computer Science, Physics and Mathematics, Linnaeus University, Växjö, Sweden.

BIOGRAPHY

H. Sinan Akşimşek received his B.Sc. degree in electrical and electronics engineering and M.Sc. degree in electronics and telecommunication engineering from Istanbul University in 2007 and Istanbul Technical University in 2010, respectively, He started his Ph.D. studies at Gebze Technical University in September, 2010. His research interests are in scattering and propagation of electromagnetic waves.